

Master's Programme in Advanced Energy Solutions

# Feasibility Study of E-methanol in the Nordic Context

---

**Miina Sivula**

Copyright © 2025 Miina Sivula

---

**Author** Miina Sivula

---

**Title** Feasibility Study of E-methanol in the Nordic Context

---

**Degree programme** Advanced Energy Solutions

---

**Major** Energy Systems and Markets

---

**Supervisor** Prof. Matti Lehtonen

---

**Advisor** Dr. Mohamed Magdeldin

---

**Collaborative partner** Sumitomo SHI FW

---

**Date** 16. December 2025

**Number of pages** 74

**Language** English

---

### **Abstract**

The energy sector is effectively decarbonizing through the large-scale deployment of renewable energy sources, such as wind and solar power. However, these renewable energy sources exhibit high variability in availability. This leads to periods of excess energy, in which supply exceeds demand, creating a need for the development of energy storage solutions. Simultaneously, hard-to-abate sectors with growing demand require additional emissions reductions in order to curb the detrimental effects of climate change.

One proposed solution is power-to-X (PtX), which involves storing excess electricity by producing the energy carrier hydrogen through electrolysis. The produced hydrogen can be further refined to various synthetic fuels, such as e-methanol. This study investigates the feasibility of combining oxyfuel carbon capture and utilization and electrolysis to produce e-methanol. A process model was created in Aspen Plus™ using CO<sub>2</sub> and H<sub>2</sub> as feedstock. The financial feasibility was evaluated by calculating the levelized cost of methanol (LCOM). A series of sensitivity analyses was conducted on capital expenses, electricity prices, side-stream revenues, renewable energy availability, and the carbon tax to assess possible future scenarios for methanol production and markets.

The plant produces 300 ktMeOH/a of high-purity e-methanol at a LCOM of 1100 €/tMeOH. The electrolyzer's capital expenses, electricity consumption, and price are primary cost drivers for the investment. These results are discussed in depth and compared to peer-reviewed studies to evaluate their feasibility under current and possible future market conditions.

---

**Keywords** Synthetic fuels, e-methanol, electrolysis, carbon capture

---

---

**Författare** Miina Sivula

---

**Titel** Genomförbarhetsstudie av e-metanol i nordisk kontext

---

**Utbildningsprogram** Advanced Energy Solutions

---

**Huvudämne** Energy Systems and Markets

---

**Övervakare** Prof. Matti Lehtonen

---

**Handledare** Tekn. Dr Mohamed Magdeldin

---

**Samarbetspartner** Sumitomo SHI FW

---

**Datum** 16. December 2025

**Sidantal** 74

**Språk** Engelska

---

### **Sammandrag**

Energisektorn har lyckats avkarboniseras i och med upptagningen av förnybara energikällor så som vind- och solex. Likväl är energikällors tillgänglighet högt varierande över dygnet och året. Detta leder till tidsperioder med överskottsenergi, där efterfrågan inte motsvarar utbudet, vilket medför behovet av att utveckla energiförvaringsmetoder. Samtidigt ökar efterfrågan inom så kallade "hard-to-abate sectors", det vill säga högutsläppande sektorer som ännu saknar lågutsläppande alternativ. Dessa sektorer är i behov av mer effektiv avkarbonisering för att motverka klimatförändringen.

En förslagen lösning är el-till-X (PtX), vilket innebär att överskottsenergi används och lagras genom att producera väte via elektrolys. Det producerade vätet kan vidareförädlas till olika syntetiska bränslen såsom e-metanol. Denna studie undersöker genomförbarheten av att kombinera oxyfuel-baserad koldioxidavskiljning med elektrolyserat väte för att producera e-metanol. En modell av processen skapades i Aspen Plus™ med CO<sub>2</sub> och H<sub>2</sub> som råmaterial. Den ekonomiska genomförbarheten mättes genom att räkna den genomsnittliga produktionskostnaden av metanol över anläggningens livslängd (LCOM). Känslighetsanalyser utfördes på kapitalkostnaden, elpriset, möjliga biproduktsintäkter, tillgången på förnybar energi samt koldioxidskatten för att utvärdera olika möjliga framtidsscenarierna för produktionen och marknaden för metanol.

Den simulerade anläggningen producerar 300 ktMeOH/a med hög renhetsgrad, med en LCOM på 1100 €/tMeOH. Elektrolysören samt elanvändningen och dess pris är de avgörande faktorerna för investeringens kostnadsnivå. Dessa resultat diskuteras i detalj och jämförs med andra vetenskapliga studier för att utvärdera deras genomförbarhet i på dagens marknader.

---

**Nyckelord** Syntetiska bränslen, väte, e-metanol, elektrolys, koldioxidavskiljning

---

## **Preface**

I would like to thank Professor Matti Lehtonen for his guidance, engaging discussions, and humor throughout the making of this thesis. I express my sincere gratitude to my instructor, Dr. Mohamed Magdeldin, for his advice, sharp questions, and especially for challenging me throughout these six months. I also want to thank Pasi Petra for his support during the writing process.

Thank you to my collaborative partner Sumitomo SHI FW, for granting me such an interesting thesis topic and trusting me to explore the emerging sector of e-fuels. A special thanks to my colleagues who have expressed sincere excitement and contributed valuable insight to this thesis.

Finally, a warm thank you to my family, friends, and housemates for their support and encouragement throughout the various stages of my academic journey. Fortunately, this journey does not end with the completion of this thesis.

Helsinki, 16.12.2025

Miina Sivula

# Contents

<b>Preface</b>	<b>5</b>
<b>Contents</b>	<b>6</b>
<b>Abbreviations</b>	<b>8</b>
<b>1 Introduction</b>	<b>9</b>
<b>2 Carbon Capture Technologies</b>	<b>12</b>
2.1 Background . . . . .	12
2.2 Pre-combustion . . . . .	13
2.3 Post-combustion . . . . .	13
2.4 Oxyfuel Combustion . . . . .	14
<b>3 Oxygen Production Technologies</b>	<b>16</b>
3.1 Oxygen Market Overview . . . . .	16
3.2 Air Separation Technologies . . . . .	17
3.2.1 Cryogenic Air Separation . . . . .	17
3.2.2 Air Separation Membranes and Swing Adsorption Units . . . . .	18
3.3 Electrolyzers . . . . .	19
3.3.1 Market Overview . . . . .	19
3.3.2 Alkaline Electrolyzer . . . . .	20
3.3.3 Proton Exchange Membrane Electrolyzer . . . . .	21
3.3.4 Anion Exchange Membrane Electrolyzer . . . . .	22
3.3.5 Solid Oxide Electrolyzer . . . . .	22
<b>4 E-methanol Production and Markets</b>	<b>23</b>
4.1 Methanol as an E-fuel . . . . .	23
4.2 Methanol Production with CO <sub>2</sub> Hydrogenation . . . . .	24
4.2.1 CO <sub>2</sub> Hydrogenation Routes . . . . .	25
4.2.2 Process Equipment and Catalysts . . . . .	27
4.3 Market Outlook . . . . .	28
4.3.1 Methanol Supply and Demand . . . . .	28
4.3.2 Cost of Methanol . . . . .	30
4.3.3 Methanol Production Incentives . . . . .	31
<b>5 Materials and Methods</b>	<b>33</b>
5.1 Process Simulation . . . . .	33
5.1.1 Electrolyzer . . . . .	34
5.1.2 E-methanol CO <sub>2</sub> Hydrogenation . . . . .	35
5.1.3 Heat Recovery and Process Integration . . . . .	36
5.1.4 Efficiencies . . . . .	38
5.2 Economic Analysis . . . . .	39
5.2.1 Capital Expenditures . . . . .	39

5.2.2	Operational Expenditures . . . . .	41
5.2.3	Levelized Cost of Methanol . . . . .	42
5.3	Sensitivity Analysis Framework . . . . .	42
5.3.1	Electrolyzer Cost and Electricity Price . . . . .	43
5.3.2	Side Stream Revenues . . . . .	43
5.3.3	Renewable Energy Availability . . . . .	44
5.3.4	Carbon Tax and Market Price . . . . .	45
<b>6</b>	<b>Results and Discussion</b>	<b>47</b>
6.1	Technical Results . . . . .	47
6.1.1	Energy Requirements . . . . .	47
6.1.2	Heat and Mass Balances . . . . .	48
6.1.3	Process Heat Integration . . . . .	50
6.1.4	Process Efficiencies . . . . .	51
6.2	Economic Results . . . . .	52
6.2.1	Capital Expenditures . . . . .	52
6.2.2	Operational Expenditures . . . . .	53
6.2.3	Levelized Cost of Methanol . . . . .	54
6.3	Sensitivity Analysis . . . . .	55
6.3.1	Electrolyzer Cost and Electricity Price . . . . .	55
6.3.2	Side Stream Revenues . . . . .	57
6.3.3	Renewable Energy Availability . . . . .	59
6.3.4	Impact of Carbon Tax on Market Prices . . . . .	62
6.4	Limitations and Suggestions for Further Research . . . . .	63
<b>7</b>	<b>Conclusions</b>	<b>65</b>

## Abbreviations

AEM	anion exchange membrane
ASU	air separation unit
BECC	bioenergy with carbon capture
BoP	balance of plant
CAPEX	capital expenditure
CCUS	carbon capture, utilization, and storage
CO <sub>2</sub> eq	CO <sub>2</sub> equivalent
CPU	CO <sub>2</sub> purification unit
DAC	direct air capture
ETS	emissions trading system
GHG	greenhouse gas
HER	hydrogen evolution reaction
IMO	international maritime organization
KPI	key performance indicator
LCOH	levelized cost of hydrogen
LCOM	levelized cost of methanol
LHV	lower heating value
LNG	liquefied natural gas
M€	million euros
MeOH	methanol
MGO	marine gas oil
MWe	Mega Watt electric
MWth	Mega Watt thermal
OER	oxygen evolution reaction
OPEX	operational expenditure
PEM	proton exchange membrane
RFNBO	renewable fuels of non-biological origin
SOE	solid oxide electrolyzer
Syngas	synthetic gas
TRL	technology readiness level
USD	United States Dollar

# 1 Introduction

As the consequences of climate change threaten current and future generations on planet Earth, powerful institutions, such as the European Union, have set targets to reduce carbon dioxide emissions. The European Union has set a target to be climate neutral by 2050 (European Union, 2021). This target includes reducing greenhouse gas (GHG) emissions by 55 %, compared to 1990 levels, by 2030. In practice, this means that by 2030, the target is to emit 2.08 GtCO<sub>2</sub>eq (European Environment Agency, 2025). In 2024, 2.91 GtCO<sub>2</sub>eq was emitted, indicating that more efforts are needed in Europe to meet the target on time.

While the energy sector is decarbonizing effectively due to the deployment of renewable energy sources, hard-to-abate sectors remain major polluters. Especially, international shipping and aviation are facing issues in reducing their emissions. Currently, domestic transport, international aviation, and international shipping sectors contribute with 27.3 %, 4.2 %, and 4.2 % of emissions in Europe (European Environment Agency, 2025). While the energy sector in general has managed to reduce its emissions by approximately half since 1990, international aviation and shipping have, in turn, increased their emissions by 124.6 % and 21.2 %, respectively. While other sectors are being electrified, hard-to-abate sectors have failed in implementing similar strategies. These sectors require alternative solutions for decarbonization to mitigate the consequences of climate change.

The rapid growth and uptake of renewable electricity, such as wind and solar, has led to a volatile energy supply (Fingrid Oyj, 2025). The volatile availability of energy has led to several issues within the energy system. For instance, grid balancing challenges and excess electricity supply have led to curtailment, meaning producers intentionally restrict the amount of power they produce, although there is capacity available (Jung and Schindler, 2020). As renewable energy has gained an increased market share and pushed prices down, high-cost baseload fossil alternatives are being pushed out of the market (Liski and Vehviläinen, 2016). To address the issue of variable supply, flexibility of energy use and different energy storage solutions are needed for demand and supply to meet.

When renewable energy is available and there is insufficient demand, the cheap excess electricity could be used to power electrolyzers to produce green hydrogen. Hydrogen could be considered an energy storage solution in these cases. The electrolyzer requires only electricity to produce hydrogen, making it a viable option for energy storage in an energy mix saturated with volatile renewable power sources.

Hydrogen, however, requires advanced technology for safe storage and has a low volumetric energy density (Akyüz et al., 2024). Therefore, the power-to-X (P2X) pathway is also extensively researched and discussed. P2X refers to the production of synthetic fuels by using excess electricity to produce hydrogen, which is further refined into another fuel, such as methanol or ammonia. These fuels, produced via a fossil-free pathway, are referred to as e-fuels and are intended to replace their fossil alternatives (IRENA, 2021).

Despite the rapid decarbonization of the energy sector, emissions also remain within sectors besides transportation. Industrial and chemical processes, such as iron, steel, cement, and other energy production facilities, contribute significantly to carbon emissions today. Industrial processes currently account for 21.6 % of emissions in the European Union (European Environment Agency, 2025). While society depends on these products, the processes that produce them require conditions such as high temperatures, which inherently lead to high carbon emissions. As other alternatives to these processes have been viably proposed, technical solutions for restricting carbon emissions are being developed. Consequently, to enable the production of these products, carbon capture of the produced emissions is being explored.

The harmful carbon emissions could be captured before being released into the atmosphere through different carbon capture methods. The CO<sub>2</sub> can then be stored or further processed to be utilized for other purposes, such as synthetic fuel production (Nema et al., 2025). Alternatively, direct air capture (DAC) involves capturing CO<sub>2</sub> directly from the atmosphere for storage or utilization. Currently, carbon capture from industrial processes is the cheaper alternative, as DAC requires highly advanced technologies due to the high dilution of CO<sub>2</sub> in atmospheric air, compared to industrial flue gases (IRENA, 2021).

Therefore, there exists potential synergies between hard-to-abate sectors and intermittent renewable energy production. Carbon dioxide emissions must be reduced from both industrial processes and transport, such as shipping and aviation. Simultaneously, there is an overflow of renewable, clean energy, which can be converted into fuel for heavy vehicles and aviation by utilizing captured carbon. If successful, this combination could reduce carbon emissions from shipping, aviation, and diverse industrial processes, while increasing the utilization rate and efficiency of renewable energy sources.

The aim of this thesis is to make a techno-economic evaluation of the production of e-methanol through the synthesis of green hydrogen and captured carbon dioxide in the Nordics and estimate the costs related to the process. In other words, to identify one efficient pathway to decarbonize hard-to-abate sectors.

The research questions are the following:

1. What is the levelized cost of producing e-methanol through oxyfuel carbon capture and electrolysis?
2. How can potential synergies with oxygen and heat be utilized within the e-methanol production process?
3. What is required from the market or production process technology for e-methanol to be financially feasible?

The thesis is based on a case study for a plant to be located in the Nordics and considers relevant European regulations. The case study is based on an existing oxyfuel circular fluidized-bed boiler operating on biomass in Sweden. The capacity of the plant is

170 MWth and 60 MWe. Modeling is carried out based on the plant's carbon dioxide emissions. The plant sizing is designed to maximize the utilization of the CO<sub>2</sub> available from the studied plant.

This thesis is structured as follows: first, Section 1 offers an introduction to the thesis. Section 2 provides an overview of different carbon capture technologies and compares their benefits and challenges. Section 3 evaluates different routes to oxygen production and analyzes the different electrolyzer types available today. Section 4 introduces different pathways for e-methanol production and discusses its current and projected market development. Section 5 describes the methodological approach. Section 6 reports and discusses the modeling and economic results as well as the sensitivities, along with the limitations and future research suggestions. Finally, Section 7 summarizes the key conclusions of the thesis.

## 2 Carbon Capture Technologies

This section provides an overview of current carbon capture technologies in the industrial context and aims to review the most suitable alternative for e-methanol production. Pre-combustion, post-combustion, and oxyfuel combustion carbon capture methods are evaluated.

### 2.1 Background

Carbon capture has become a vital technology solution for reducing GHG emissions from industrial processes and power plants (Obi et al., 2025). Carbon capture, utilization, and storage (CCUS) refers to capturing carbon emissions from fuel combustion before the harmful gases enter the atmosphere. In the capture process, CO<sub>2</sub> is separated from various exhaust gases and then compressed and transported, for instance, by pipeline or ship. Carbon capture itself does not prevent carbon emissions from entering the atmosphere; it simply postpones it if the carbon is not captured again when the utilized CO<sub>2</sub> is used (Nema et al., 2025).

Figure 1 shows the three primary technologies for carbon capture, namely oxyfuel combustion, pre-combustion, and post-combustion carbon capture. Each has distinct characteristics that suit different conditions, for instance, differences in gas stream temperature and pressure, and CO<sub>2</sub> concentration.

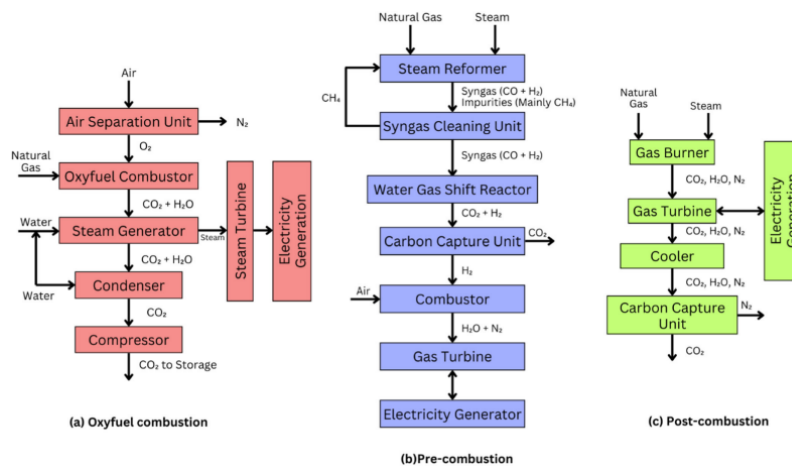


**Figure 1:** Oxyfuel, pre-combustion and post-combustion carbon capture (Obi et al., 2025)

Direct air capture (DAC) is an additional technology that captures carbon dioxide directly from the atmosphere. The concentration of CO<sub>2</sub> in atmospheric air is lower than in industrial flue gases, making it the most energy-intensive and expensive alternative for carbon capture (IEA, 2022). As the focus is on capturing point source emissions from power production and industrial processes, DAC technology is outside the scope of this thesis.

## 2.2 Pre-combustion

In pre-combustion capture, CO<sub>2</sub> is separated from H<sub>2</sub> in a fuel before combustion. Carbon dioxide is captured, and hydrogen can be used as an energy carrier for other purposes. Pre-combustion technology can be applied to various types of fuel, including biomass, coal, and natural gas (Obi et al., 2025).

In the pre-combustion process, the fuel is converted into a synthetic gas (syngas) through gasification of solid fuels or via reforming at high pressure and temperature with limited oxygen. First, the converted syngas is mainly a mixture of CO and H<sub>2</sub>, which is then subjected to a water-gas shift reaction to increase hydrogen yield. When CO is exposed to H<sub>2</sub>O steam with a catalyst, it reacts into CO<sub>2</sub> and H<sub>2</sub>. Carbon dioxide is often separated from the mixture using physical or chemical absorbents, adsorption, or different advanced membranes (Hamedani et al., 2025; Obi et al., 2025). Many other separation methods are also currently under development (Hamedani et al., 2025). After pre-combustion processing, carbon dioxide has a high partial pressure (Vaziri et al., 2024), making the CO<sub>2</sub> separation process relatively easy. The separated and captured CO<sub>2</sub> can be further processed, transported, and utilized or sequestered.

The advantages of pre-combustion include a high capture efficiency of 90 %. The concentration of CO<sub>2</sub> is relatively high, exceeding 20 % in syngas (Hamedani et al., 2025). Simulations by Obi et al. (2025) suggest that the captured CO<sub>2</sub> can reach purities up to 97.0 %. Because of the high concentration, the energy demand for carbon separation and capture is relatively low, allowing for lower costs. However, Skorek-Osikowska et al. (2017) compared a conventional power plant with and without pre-combustion carbon capture, and concluded that the inclusion of pre-combustion carbon capture reduced the net energy efficiency for electricity production by 17 percentage points.

## 2.3 Post-combustion

Post-combustion carbon capture is an established technology in which CO<sub>2</sub> is separated from the exhaust gas after the combustion has taken place in a power plant or industrial process. After combustion, the particular matter, SO<sub>2</sub>, and NO<sub>x</sub> are removed from the flue gas. Carbon dioxide is then separated and purified through processes such as solvent-based absorption, adsorption, membrane separation, and chemical looping (Yusuf et al., 2023). If needed, the separated CO<sub>2</sub> can then be further purified to meet the requirements of utilization or sequestration, after which it can be transported to the next destination.

The advantage of post-combustion carbon capture is its ability to be retrofitted into existing plants with relatively minor modifications. It is also compatible with several types of fuel, such as natural gas and biomass (Obi et al., 2025).

However, this technology has several drawbacks with respect to CO<sub>2</sub> concentration and costs. The CO<sub>2</sub> content of the flue gas is low, ranging between 3-15 % for different technologies, which complicates and increases the operating and maintenance costs

of the separation process (Hamedani et al., 2025). The CO<sub>2</sub> concentration of carbon dioxide captured is also relatively low, approximately 93.0 % (Obi et al., 2025). Moreover, the high energy intensity of the process is suggested to reduce the efficiency of power produced by approximately 12 percentage points (Skorek-Osikowska et al., 2017).

## 2.4 Oxyfuel Combustion

Oxyfuel combustion is a carbon capture technology that creates a more concentrated flue gas to simplify the CO<sub>2</sub> separation process. It can be used in various applications, including power generation and industrial processes such as steelmaking. Nearly pure oxygen is used as the combustion environment in oxyfuel combustion instead of conventionally used air. This produces product gas rich in CO<sub>2</sub> and water vapor, enabling efficient separation and capture (Nema et al., 2025). To control combustion chamber temperature, some flue gas can be recirculated into the boiler. The rest of the flue gas is condensed to remove water vapor, then compressed and further purified for storage or utilization (Hamedani et al., 2025).

To create a purer combustion environment and therefore purer flue gas, air separation units (ASU) and CO<sub>2</sub> purification units (CPU) are typically used. The ASU separates oxygen from air, which is then fed into the combustion chamber to create a pure combustion environment and concentrated flue gas. The concentrated flue gas is then further cleaned by the CPU after combustion. The CPU process includes purification steps to remove residual water vapor, oxygen, and other non-condensables. The targeted purity of oxygen in the combustion chamber is usually 95 % and above, depending on the process (Hamedani et al., 2025). Optimizing the CPU with an ASU can enable cost-effectiveness. A combustion environment enriched in O<sub>2</sub> produces a flue gas with a higher CO<sub>2</sub> concentration, thereby reducing the processing requirements of the CPU (Nema et al., 2025).

Although ASUs are the conventionally used oxygen production technology today, it is important to recognize the oxygen produced by the electrolyzer in the context of e-methanol production. Air separation units and electrolyzers are compared further in Section 3.

Similar to post-combustion, oxyfuel can accommodate various fuel types, including biomass, coal, and natural gas. It is merited for its high efficiency in CO<sub>2</sub> capture and up to 70 % reduction in nitrous oxide emissions due to the lower levels of nitrogen in the combustion chamber. It also emits less particle matter, sulfur dioxide, and other pollutants per unit of CO<sub>2</sub> captured than pre- and post-combustion (Obi et al., 2025).

However, oxyfuel is challenged by high investment costs compared to pre- and post-carbon capture. Moreover, the specific energy consumption of the ASU decreases the efficiency of the oxyfuel power plant and carbon capture process (Brigagão et al., 2025). Skorek-Osikowska et al. (2017) estimates that the efficiency losses in oxyfuel combustion are approximately 8 percentage points, which is the least efficiency loss compared to pre- and post-combustion carbon capture. On the other hand, the

cryogenic ASU, which is most commonly used in oxyfuel today, is a costly technology. It can contribute up to 14 % of the overall cost of oxyfuel production (Hamedani et al., 2025). Furthermore, Huang et al. (2022) report issues in corrosiveness due to absorbents used in the CO<sub>2</sub> separation process in oxyfuel combustion. Despite these challenges, Hamedani et al. (2025) argue that oxyfuel combustion may be the most favorable option compared to post- and pre combustion carbon capture.

## 3 Oxygen Production Technologies

This section analyzes the production methods and requirements for oxygen used in oxyfuel combustion. First, it reviews the current global oxygen demand, after which air separation units and different electrolyzer types are reviewed and compared.

### 3.1 Oxygen Market Overview

Oxygen demand is prominent worldwide because it is used in various sectors. Eckl et al. (2025) defines the important oxygen applications as iron and steel, cement, pulp and paper, wastewater treatment, medical care, and ceramic industries.

The iron and steel industry is the largest oxygen consumer in the world today. Pure oxygen is used to remove impurities from cast iron through oxidation (Eckl et al., 2025). Using oxygen in blast or electric arc furnaces also improves the efficiency of the process and the properties of the resulting steel (Kato et al., 2005). Oxyfuel combustion has also gained popularity in cement and glass production. Cement production accounts for 7 % of global emissions, which oxyfuel combustion and carbon capture could significantly decrease. Glass production has also adopted oxyfuel combustion for the glass melting process. Oxyfuel combustion is 10-20 % more efficient than traditional glass melting furnaces, making it an attractive option (Eckl et al., 2025).

Even the ceramic industry faces pressure to decarbonize, for which oxyfuel also shows potential. However, oxyfuel combustion in the ceramics industry is not yet widely used. On the other hand, the pulp and paper industry has adopted the use of oxygen to reduce reliance on harmful chlorine-based bleaching chemicals. Wastewater treatment is also considered a potential oxygen consumer in the future. Wastewater is conventionally cleaned with air to degrade organic matter, but it is more efficient when pure oxygen is used. Medical care also requires oxygen outside of industrial applications. Healthcare uses high-purity oxygen for the treatment of many different health problems, including respiratory diseases. Oxygen used in healthcare has strict purity level restrictions, up to 99.5 % v/v. (Eckl et al., 2025)

The predicted upswing in electrolyzers is projected to impact oxygen markets significantly. Currently, there are 215 water electrolyzers in operation or under construction in Europe. These electrolyzers have a total electrical capacity of 3 200 MW and an estimated annual total hydrogen production rate of 530 kt (European Hydrogen Observatory, 2025b). By stoichiometry, it can be calculated that these electrolyzers also produce oxygen, 8 times the mass of the produced hydrogen. This translates to 4.25 Mt of oxygen annually, while the current demand of oxygen in Finland alone is estimated at 1.3 Mt (Hurskainen, 2017). The oxygen market competition is therefore expected to become highly saturated, pushing prices down. For reference, the market price of industrial oxygen in 2014 was approximately 73 €/tO<sub>2</sub> (Hurskainen, 2017).

## 3.2 Air Separation Technologies

This section provides an overview of air separation technologies that are considered commercially mature and have a high technology readiness level (TRL). Oxygen can be separated from air by splitting air into its main components. Air consists of 78 % nitrogen, 21 % oxygen, and 1 % other gases, including argon. The reviewed technologies are cryogenic air separation, air separation membranes, and swing adsorption units.

### 3.2.1 Cryogenic Air Separation

The cryogenic oxygen production process is a well-established technology, which can produce oxygen with over 99 % purity at high volumes. The highest rates are up to tens of thousands of tonnes of oxygen per day. The trade-off with this technology is its extremely high energy intensity per tonne of oxygen produced. However, to achieve high production volumes and purity levels, cryogenic separation has been suggested to be the best available technology (e.g. Higginbotham et al., 2011; Jha and Gaur, 2022)

Cryogenic air separation is based on fractional distillation of air to separate it into oxygen and nitrogen. Figure 2 shows a schematic of a typical air separation process (Tesch et al., 2019). The main components of the ASU are the air compressor, air purification, heat exchangers, and distillation columns. The process begins with a compressor collecting ambient air, which is compressed from 1 bar to 6 bar. This is the pressure at which most of the process will operate to enable smooth handling by the adsorption unit and heat exchanger. The air is then cooled down to cryogenic temperatures in the heat exchanger before entering the distillation column for separation. Based on their respective boiling points, oxygen and nitrogen are distilled and separated into distinct containers (Tesch, et al., 2019). If ultra-high purity is required, argon can also be separated in a separate distillation column.

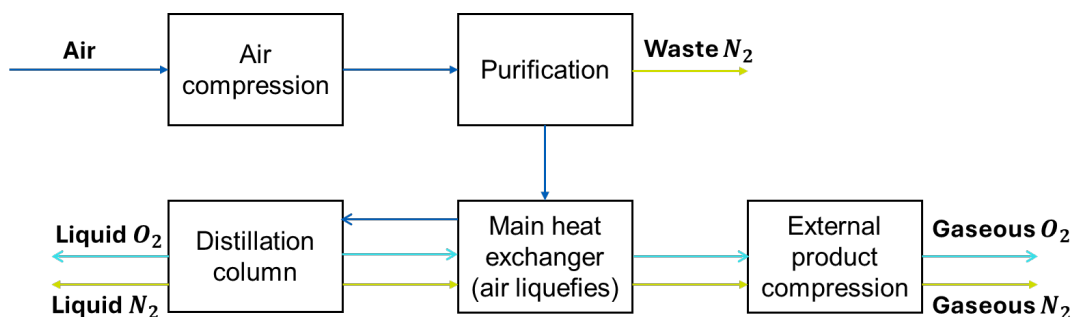


**Figure 2:** Schematic of the typical components of an ASU (Tesch et al., 2019).

The distillation system consists of a high-pressure and a low-pressure column. First, it enters the high-pressure column at 6 bar, at which the boiling point of oxygen is -166 °C and nitrogen is -178 °C. Oxygen is partially liquefied and creates an oxygen-rich mixture at the bottom of the column, whereas a nitrogen-rich gas is collected at the top. For further purification, the mixtures are sent to the low-pressure column, at

approximately 1 bar, at which the boiling points of oxygen and nitrogen drop to  $-183\text{ }^{\circ}\text{C}$  and  $-200\text{ }^{\circ}\text{C}$ , respectively. At this temperature, nitrogen also starts to liquefy and is further separated from oxygen.

When nitrogen has been separated and sent forward, the oxygen-rich liquid can be sent further into the argon distillation column. If the required purity of oxygen is above 96 %, as often in oxyfuel combustion or medical purposes, it must be distilled separately from argon (Li et al., 2024). Oxygen and argon have similar ambient boiling points,  $-183\text{ }^{\circ}\text{C}$  and  $-186\text{ }^{\circ}\text{C}$ , respectively. The proximity of the boiling points necessitates a separate argon distillation column to achieve the desired purity level. Once oxygen and argon have reached their respective required purities, they are sent to cryogenic containers for storage and transportation.

Process optimization is crucial for an ASU integrated into an oxyfuel combustion power plant, as every unit of power consumed by the ASU decreases the total energy efficiency of the power plant. For instance, the company Air Liquide currently offers high-purity ASU with energy intensities ranging from 160-600 kWh/tO<sub>2</sub> (Air Liquide, 2017). This is consistent with current research findings on achievable energy intensities (e.g. Belaissaoui et al., 2014; Mehrpooya et al., 2020). However, achieving an energy intensity as small as 160 kWh is described as extremely ambitious by (Belaissaoui et al., 2014), as the inevitable compression and cooling steps of the process are highly energy-consuming (Cai et al., 2024). Moreover, Mehrpooya et al. (2020) propose a simulated energy intensity of 300 kWh/tO<sub>2</sub> for oxygen purities above 99 %.

As the process is highly energy-intensive, the production costs are sensitive to local electricity and grid prices. However, despite the high energy consumption, the cost of production can be relatively low, especially for large-scale production. The cost of producing 95 % pure oxygen on a large scale, more than 300 tO<sub>2</sub>/d, could be as low as USD 45/tO<sub>2</sub> (Cai et al., 2024).

Due to the nitrogen production from ASUs, they are more suitable for e-ammonia production than for e-methanol production. However, combined with oxyfuel and electrolyzers, ASUs could serve as a backup solution for oxygen production for the boiler.

### **3.2.2 Air Separation Membranes and Swing Adsorption Units**

Conventional membrane air separation produces low-purity oxygen, often termed oxygen-rich air, as its oxygen purity is around 45 %. These commercial membranes are typically polymer-based. However, researchers are currently developing new membranes of ceramic or perovskite to deliver higher-purity oxygen. These non-commercial membranes have shown 95-99 % oxygen purity. However, the scale of production is much smaller than that of cryogenic air separation, ranging from 1 to 50 tO<sub>2</sub>/day. (Micari and Agrawal, 2022)

The swing adsorption units are mature technologies based on the adsorption of nitrogen out of the air. It is based on a two-bed column that is packed with an adsorbent made

of natural or synthetic materials, usually zeolites (Jha and Gaur, 2022). One of the beds is in the adsorption state and the other in the desorption state, meaning it is in the regeneration state (Eckl et al., 2025). There are several types of swing adsorption regeneration, either based on pressure or heat differences. The most widely used swing adsorption systems are pressure swing adsorption, vacuum pressure swing adsorption, and temperature swing adsorption. The oxygen purity levels of swing adsorption are usually approximately 95 % and are favored for small-scale production, around 20-100 tO<sub>2</sub>/day (Eckl et al., 2025). However, the current energy intensity of high-purity swing adsorption has shown very high energy intensities, up to 889 kWh/t O<sub>2</sub>. However, the energy intensity is predicted to decrease in the future through technological development (Eckl et al., 2025).

The literature reviewed for this thesis indicates that many alternative oxygen separation technologies to cryogenic air separation could be beneficial to use in natural gas cycles (e.g., Alrebei et al., 2022; Lube et al., 2025). However, not many studies have shown alternatives to cryogenic oxygen production for biomass-based oxyfuel fluidized bed boilers.

### 3.3 Electrolyzers

This section discusses current markets and technological advancements in electrolyzer technology, highlighting potential electrolyzer types and configurations for hydrogen and oxygen production.

#### 3.3.1 Market Overview

Electrolysis is a well-established technology that splits water into hydrogen and oxygen. It was discovered as early as the beginning of the nineteenth century (Niu et al., 2025). Shortly after the discovery, the development of electrolyzers for hydrogen production stalled because fossil-based hydrogen production dominated due to its cost efficiency. However, with the need to decarbonize energy production, electrolysis has again gained attention in research and industry in the 21st century.

Although hydrogen is usually the desired product from the electrolyzer, the byproduct oxygen could also be utilized, for instance, in oxyfuel carbon capture. The water-splitting reaction in the electrolyzer is shown in Equation 1. In the process, an electric current is induced in water H<sub>2</sub>O, which is decomposed into hydrogen H<sub>2</sub> and oxygen O<sub>2</sub>. This covers two half reactions, the hydrogen evolution reaction (HER) and the oxygen evolution reaction (OER) (Niu et al., 2025).



These reactions produce two moles of gaseous hydrogen and one mole of gaseous oxygen. The relative mass of the oxygen produced is remarkable. The molar masses of the elements are H<sub>2</sub> = 2.016 g/mol and O<sub>2</sub> = 32.00 g/mol. The molar mass of oxygen

produced is almost eight times larger than the molar mass of hydrogen. Although releasing the oxygen into the atmosphere is claimed to be harmless, there are potential use cases for the produced oxygen, motivating its storage as well (Eckl et al., 2025).

Electrolyzers consist of an electrolyte, the electrodes, a separator or membrane, and the electric circuit. The oxygen and hydrogen are collected at the electrodes, that is, the anode or the cathode. The type of electrolyte used and the working principle of the electrodes depend on the type of electrolyzer.

The four leading electrolyzers today are alkaline, proton exchange membrane (PEM), anion exchange membrane (AEM), and solid oxide electrolyzer (SOE). The biggest differences are in the operating temperature of the electrolyzers and the electrolyte type. Of these four, the alkaline electrolyzer is the most mature and commercialized technology. The PEM electrolyzer has been increasingly deployed recently as well, but at higher costs than the alkaline electrolyzer. The AEM and the SOE are still mainly in the research and development phase. AEM shows much potential in combining the flexibility of PEM with the low material costs of alkaline. Moreover, SOE is considered a technology with enormous future potential because of its energy efficiency (Akyüz et al., 2024). Table 1 summarizes the key components and conditions of the four electrolyzers.

**Table 1:** Comparison of different electrolysis technologies (Şahin, 2024; Aminaho et al., 2025; Deloitte, 2021)

Attribute	Alkaline	PEM	AEM	Solid Oxide
Operating temperature (°C)	70–90	40–80	50–80	500–900
Operating pressure (bar)	1–30	<70	<35	1
Stack lifetime (h)	80 000	40 000–60 000	2 000–8 000	20 000–30 000
Fuel Efficiency (%)	60–70	60–70	50–65	70–90
CAPEX (USD/kW)	750–1400	800–1800	–	800–2300 (estimated)
LCOH (USD/kg)	2.9–6.5	2.3–7.5	1.5–5.0 (modeled)	2.5–5.0 (modeled)

The levelized costs of hydrogen can be used to estimate the levelized cost of oxygen by allocating all costs to the oxygen production. As for every kilogram of hydrogen produced in electrolysis, approximately 8 kg of oxygen is produced; it can be calculated that the cost of oxygen produced in an alkaline electrolyzer would range between USD 356–815/t O<sub>2</sub>. For PEM, the equivalent cost for oxygen produced would range between USD 293–940 /t O<sub>2</sub>. The difference is enormous when compared to the cost of oxygen from cryogenic air separation of USD 45 /t O<sub>2</sub> (Cai et al., 2024). The electrolyzer can be considered inefficient solely as an oxygen production technology. Therefore, when choosing the electrolyzer size it should be designed according to the hydrogen demand and not according to oxygen demand.

### 3.3.2 Alkaline Electrolyzer

Alkaline electrolysis is the most commercially developed and applied water electrolyzer today. It uses a liquid alkaline electrolyte, typically high-concentration potassium

hydroxide KOH and non-precious metal catalysts, such as nickel and iron (Aminaho et al., 2025). Furthermore, the alkaline electrolyzer provides a long lifetime with a relatively high fuel efficiency of 60-70 %, and operates at low temperatures of 60-80 °C (Aminaho et al., 2025). It has a relatively low current density of up to 0.6 A/cm<sup>2</sup> and low pressure (Trattner et al., 2021). Aminaho et al. (2025) suggests that the required water to hydrogen ratio is 8.9 kgH<sub>2</sub>O/kgH<sub>2</sub>. The water-to-oxygen ratio is then 1.1 kgH<sub>2</sub>O/kgO<sub>2</sub>.

Alkaline is currently the most cost-efficient electrolysis solution. Deloitte (2021) estimated its costs at USD 750-1400/kW, but Gulay et al. (2025) estimates higher costs, approximately USD 1800/kW. Aminaho et al. (2025) reviewed combinations of different energy sources with the alkaline electrolyzer. They concluded that alkaline always delivers a relatively low levelized cost of hydrogen (LCOH) for geothermal, biomass, hybrid PV-wind, or grid power when it is fueled at a high capacity factor and with moderate water treatment.

However, the suggested challenge with the alkaline electrolyzer is to combine it with intermittent renewable sources, as the volatility of the energy supply leads to greater degradation of the system. Electricity typically accounts for most of the LCOH in alkaline systems. Baseload energy sources that are capable of providing constant power output deliver lower hydrogen costs than intermittent renewables, such as solar or wind. (Aminaho et al., 2025)

### 3.3.3 Proton Exchange Membrane Electrolyzer

The PEM electrolyzer is one of the most popular emerging water splitting technologies. Its benefit is its highly dynamic and fast response time (Trattner et al., 2019), making it highly adaptable to intermittent renewable energy sources. This is because the proton transport across the polymeric membrane responds quickly to power fluctuations (Ursua et al., 2012). The primary mechanism is proton conduction with a solid polymer membrane and noble-metal catalysts, such as platinum or iridium. It operates at high current densities, between 1.5-2.0 A/cm<sup>2</sup> and fuel efficiencies of 60-70 % (Akyüz et al., 2024).

Similarly to alkaline, the PEM operates at low temperatures, 50-80 °C. It can also deliver high-purity hydrogen and oxygen. For oxygen production, it can deliver purities up to 99.0 % (Eckl et al., 2025), which is a clear benefit when further refining both oxygen and hydrogen. Aminaho et al. (2025) estimated a similar water to hydrogen ratio of 8.9 kgH<sub>2</sub>O/kgH<sub>2</sub> as for alkaline. However, because the PEM requires rare metals for catalysts, it is a more costly alternative than alkaline. In 2025, Gulay et al. (2025) estimates the CAPEX at USD 2000/kW, while Deloitte (2021) suggested USD 800-1800/kW in 2020.

Furthermore, its challenge is its requirement for high-purity water at  $\leq 0.1 \mu\text{S}/\text{cm}$ , which requires a more extensive water treatment (Aminaho et al., 2025). The PEM electrolyzer has a shorter operational lifespan at approximately 60 000 hours. If the water-purity requirements are not met, this could further accelerate the degradation.

Another challenge is its reliance on noble metals, which exposes it to supply chain risks. Aminaho et al. (2025) still conclude that PEM remains a relevant choice in space-limited applications with a volatile renewable power supply and strict gas purity requirements.

### **3.3.4 Anion Exchange Membrane Electrolyzer**

The AEM electrolyzer is an emerging technology still in its early stages of development. The AEM operates in an alkaline electrolyte such as KOH or NaOH, but uses a solid polymer that conducts anions. This allows for the use of low-cost catalysts nickel, cobalt, and iron (Aminaho et al., 2025). Its operating temperature ranges 40-90 °C, and it has a moderate efficiency of 50-60 % (Akyüz et al., 2024). It is more resilient to a low-purity water supply than the PEM electrolyzer (Aminaho et al., 2025). However, similar to PEM, its estimated CAPEX is still USD 2000 /kW (Gulay et al., 2025).

The AEM faces significant challenges in commercializing. It requires further development in its membrane durability and load conductivity. Moreover, it is challenged by chemical degradation in long-term operation. Although it is currently less efficient and has a shorter lifetime than alkaline and PEM, it is still considered a promising technology for combining low costs with high efficiency in the future. (Aminaho et al., 2025)

### **3.3.5 Solid Oxide Electrolyzer**

The solid oxide electrolyzer differs from the other technologies by its high temperatures of 500-900 °C (Aminaho et al., 2025) or even up to 1000 °C (Trattner et al., 2019). It is still an emerging, non-commercial technology, but it could reach the highest efficiencies of all electrolyzers, up to 90 %. Its high efficiency is due to its ability to split water using both electrical and thermal energy (Aminaho et al., 2025). Its electrolyte is a solid ceramic-like material, often O<sub>2</sub> or H<sup>+</sup> (Akyüz et al., 2024) operating at 1 bar (Şahin, 2024). Currently, its scalability is predicted to be low to moderate, which is why it could be more suitable for smaller industrial processes. For oxygen, it can deliver a very high purity of up to 99.5 %.

The solid oxide electrolyzer is a nascent technology that must overcome many challenges before becoming commercial. Its most significant issues are stack degradation due to thermal stress, high materials expenses, and insulation (Aminaho et al., 2025). It is less favorable to use with purely electrical sources, such as solar PV, but is more efficient when operated with a stable thermal power input. For instance, concentrated solar power has been shown to enhance the economic viability of the solid oxide electrolyzer (Aminaho et al., 2025).

## 4 E-methanol Production and Markets

This section provides an overview of e-methanol production via CO<sub>2</sub> hydrogenation along with the current market conditions' impact on its deployment. Different pathways for CO<sub>2</sub> hydrogenation and available equipment are reviewed, and the market dynamics and current regulations are presented.

### 4.1 Methanol as an E-fuel

Electrofuels, also known as e-fuels, such as e-methanol, are emerging as a method of decarbonizing industries that are challenging to electrify (IEA, 2024). E-fuels can be produced from hydrogen from renewable electricity and captured CO<sub>2</sub> and are considered a sustainable replacement for fossil fuels. Production is often referred to as power-to-X, because the hydrogen used is produced from excess renewable electricity through electrolysis. The e-fuel is then created by combining green hydrogen with CO<sub>2</sub> captured from, for example, industrial processes. E-fuels exist in various forms, but e-methanol has some advantages compared to other alternatives, such as hydrogen, e-ammonia, e-gasoline, e-diesel, and liquefied natural gas (LNG) (IRENA, 2021; Ravi et al., 2023).

Methanol (MeOH) is an advantageous fuel because it has a relatively high volumetric energy density and is liquid at ambient temperature and pressure. In contrast, since hydrogen on its own has a very low volumetric energy density, it must be stored at high pressures of 350-700 bar or at an extremely low temperature of -253 °C (IRENA, 2021). This makes storing hydrogen an energy-intensive process. Furthermore, LNG and ammonia also require negative temperatures for storage, -162 °C and -34 °C, respectively. However, methanol is a liquid alcohol under standard ambient conditions, easy to store, handle, and transport, due to its melting point of -97.6 °C and boiling point of 64.6 °C (IRENA, 2021). Thus, e-methanol shows clear advantages in handling and transport among emerging e-fuels.

Methanol is often classified in different colors, as Figure 3 shows. Green methanol is produced entirely from renewable sources, such as biomass, wind, solar, and geothermal energy, and does not include fossil fuels. The blue methanol production process uses fossil fuels with carbon capture. Gray methanol is produced with natural gas reforming, whereas brown methanol is produced through coal gasification (IRENA, 2021). Green and blue methanol production routes have the lowest global warming potential, while gray and brown are highly carbon-intensive.

Currently, almost all methanol is produced from fossil fuels. Gray methanol accounts for 65 % of methanol production, and brown methanol accounts for 35 % today (Tabibian et al., 2023). In 2021, only 0.2 % of the methanol produced worldwide was classified as renewable, among which it was mainly bio-methanol (IRENA, 2021). However, IRENA (2021) expects a progressive shift towards renewable methanol, estimating 250 Mt of e-methanol production and 135 Mt of biomethanol production by 2050. Renewable methanol production could reduce carbon dioxide emissions by

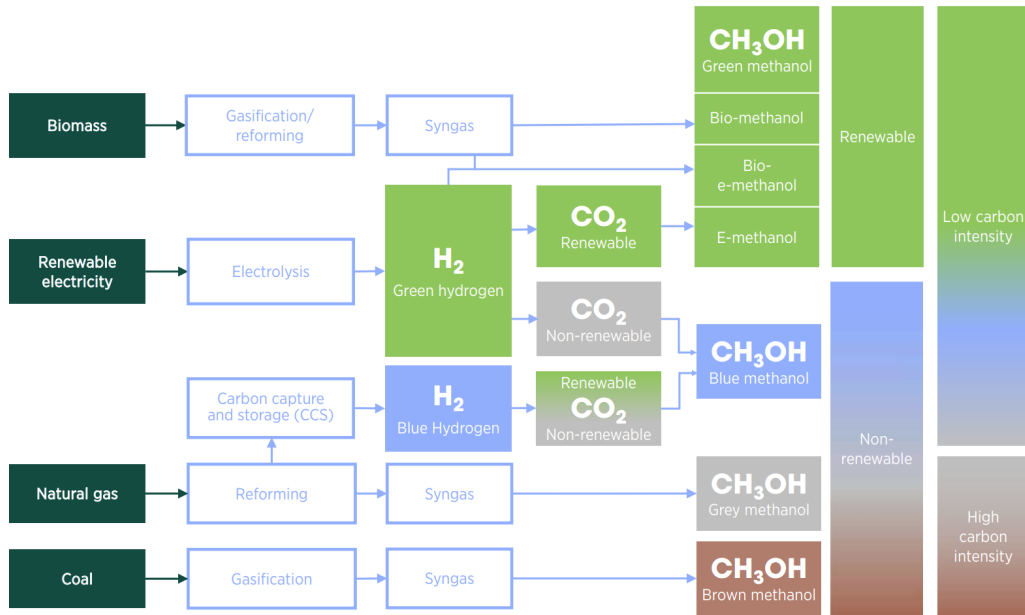


**Figure 3:** Production routes for methanol (IRENA, 2021).

95 % and nitrogen oxide emissions by up to 80 %, compared to the production of conventional fuels (Tabibian et al., 2023).

## 4.2 Methanol Production with CO<sub>2</sub> Hydrogenation

The production of e-methanol by CO<sub>2</sub> hydrogenation involves a chemical process, in which the captured CO<sub>2</sub> reacts catalytically with green H<sub>2</sub>. The reaction requires a sufficient pressure and temperature, as well as an adequate catalyst to be activated (Marques et al., 2024). In addition to the reaction requiring high heat, the reaction itself is exothermic, generating heat.

The reaction follows Equations 2, 3, and 4. The complete reaction includes one mole of carbon dioxide and three moles of hydrogen, which react to form methanol and water. However, the process follows two steps: the first is the reverse water-gas shift (RWGS) reaction, and the second is CO hydrogenation. In the first reaction, one mole of carbon dioxide reacts with one mole of hydrogen to create carbon monoxide and water, according to Equation 3. The second reaction involves the reaction of one mole of carbon monoxide with two moles of hydrogen to create methanol, according to Equation 4. Thus, the complete reaction produces both CH<sub>3</sub>OH and H<sub>2</sub>O.



#### 4.2.1 CO<sub>2</sub> Hydrogenation Routes

The CO<sub>2</sub> hydrogenation reaction can be performed in practice in multiple ways. The two main competing processes are direct and indirect CO<sub>2</sub> hydrogenation (Samimi et al., 2017; Zhong et al., 2020). The direct CO<sub>2</sub> reaction process uses one type of reactor, while the indirect process uses two different reactors. In the direct CO<sub>2</sub> hydrogenation process, the chain of reactions according to Equations 3 and 4 is induced in one reactor almost simultaneously. The indirect CO<sub>2</sub> hydrogenation process, on the other hand, uses a separate reactor for the RWGS reaction, after which the reacted syngas is fed into another reactor, in which the methanol is produced. The one-stage process is based on recycling the unreacted gases back into the reactor. In contrast, the multi-stage process feeds the unreacted gases into another similar reactor to increase the total yield of the process.

Figure 4 shows a schematic of a one-stage direct CO<sub>2</sub> hydrogenation process. In the one-stage reactor, CO<sub>2</sub> and H<sub>2</sub> are fed through a heat exchanger to reach the desired temperature of the reactor. After the reactor stage, the mixture is separated into one methanol blend stream and one unreacted gas stream. The unreacted stream mainly contains H<sub>2</sub>, CO, and CO<sub>2</sub>, which are recycled back into the reactor. (Samimi et al., 2017)

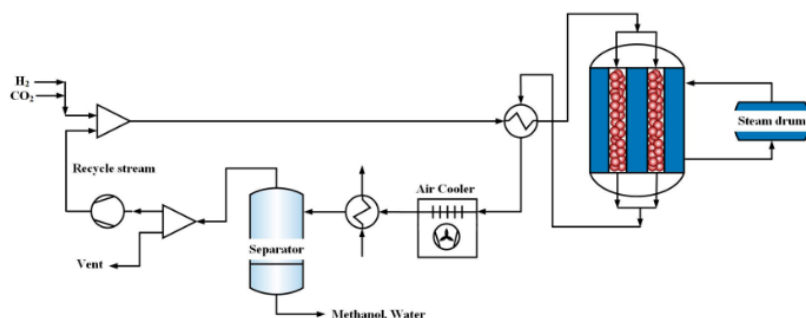


**Figure 4:** One-stage methanol reactor for direct CO<sub>2</sub> hydrogenation (Samimi et al., 2017).

An example of a multi-stage direct CO<sub>2</sub> hydrogenation process is shown in Figure 5. In this process, the remaining unreacted gases are fed to the next reactor rather than recycled back into the same process. When the mixture leaves the reactor, it is separated from methanol and water in the flash drum before continuing. The remaining mixture is then fed through a compressor and heat exchanger to reach the desired temperature and pressure for the next reactor. After the last reactor, the mixture is separated into one stream of unreacted gases and one with a mixture of methanol and water, which is then separated to produce high-purity methanol.

When comparing the multi-stage system with three reactors with a single-stage system, Samimi et al. (2017) suggest that the three-staged reactor model yields a higher CO<sub>2</sub> conversion rate and methanol production rate than the one-stage reactor model. However, the requirement of multiple reactors involves higher capital costs for the system.

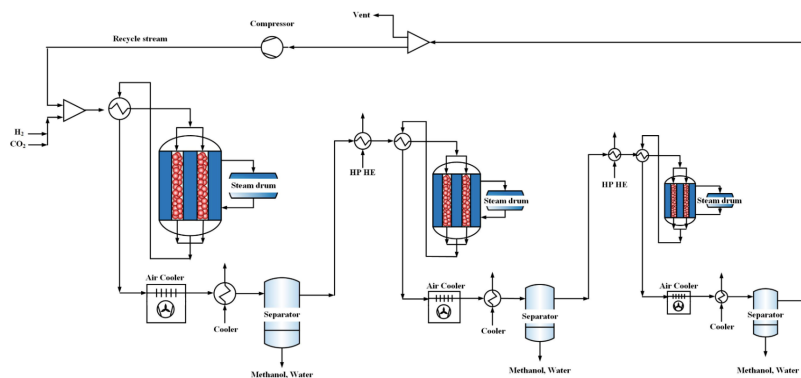


**Figure 5:** Schematic of three-stage CO<sub>2</sub> hydrogenation (Samimi et al., 2017).

The other proposed process, indirect CO<sub>2</sub> hydrogenation, involves different reactors for activated reactions. This method uses different catalysts in each reactor to more efficiently activate the desired reaction pathway. Two examples of catalysts applied in the RWGS reactor and the methanol synthesis reactor are Zn/Al<sub>2</sub>O<sub>4</sub> and Cu/ZnO/ZrO<sub>2</sub>/Ga<sub>2</sub>O<sub>3</sub>, respectively (Zhong, et al., 2020).

Figure 6 shows a flow diagram of the indirect CO<sub>2</sub> hydrogenation process. H<sub>2</sub> and CO<sub>2</sub> are fed into the RWGS reactor, where part of the CO<sub>2</sub> reacts into CO and H<sub>2</sub>O. After this, the mixture is compressed to accommodate the next reactor and H<sub>2</sub>O is removed. The remaining CO, CO<sub>2</sub>, and H<sub>2</sub> continue further through compressors and a cooler to the methanol synthesis reactor. Zhong et al. (2020) argue that the two-step process yields a higher methanol yield (over 66 %) than direct hydrogenation, due to the immediate removal of water.

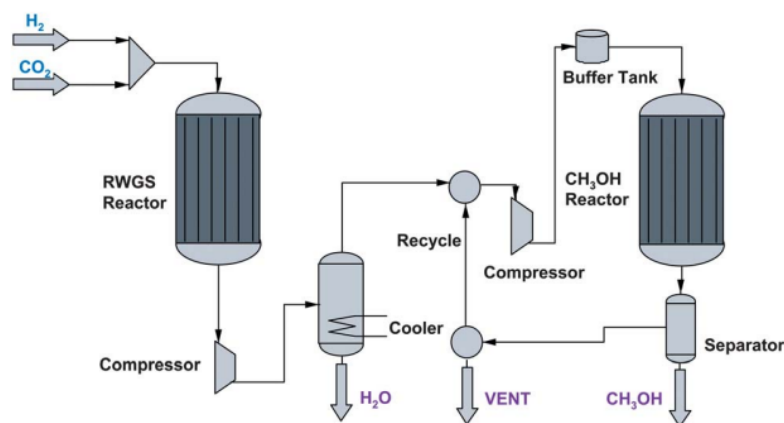


**Figure 6:** Simplified diagram of the indirect CO<sub>2</sub> hydrogenation process (Centi et al., 2013).

Currently, the literature on CO<sub>2</sub> hydrogenation can be roughly divided into two types of processes: the Kiss et al. (2016) and Perez-Fortes et al. (2016) models. Their main differences are in the hydrogen feed system. In the Kiss model, the hydrogen stream is fed directly with the recycle stream as shown in Figure 7. Perez-Fortes et al. (2016)

propose that the hydrogen feed is mixed with the CO<sub>2</sub> feed before entering the reactor. Although Kiss et al. (2016) show better results in methanol yield, the Perez-Fortez et al. (2016) model shows viable results for a large-scale process.

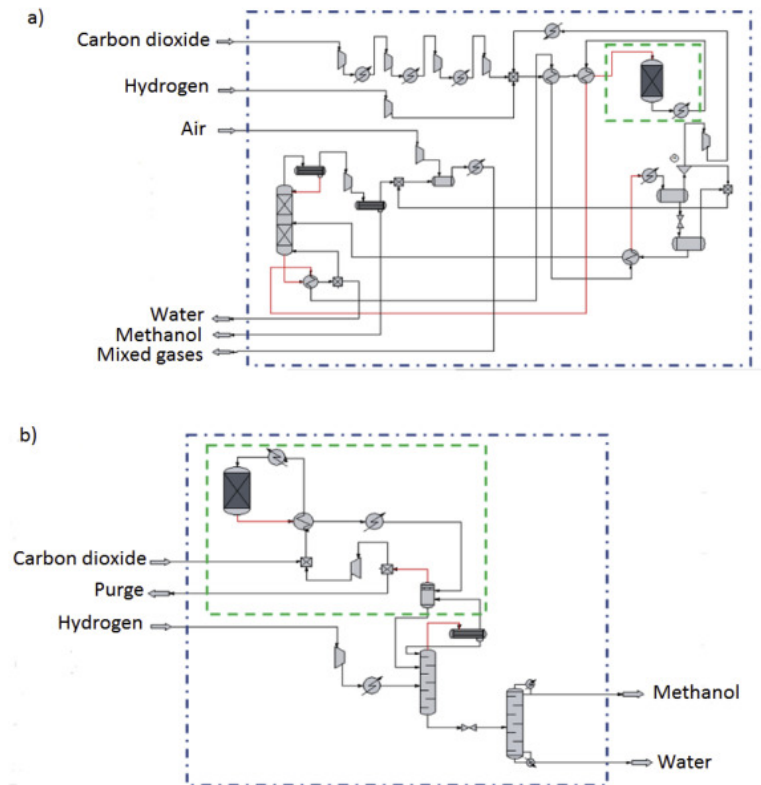


**Figure 7:** a) Process model by Perez-Fortez et al. (2016) b) Process model by Kiss et al. (2016). Graphical presentation from Leonzio et al. (2019).

#### 4.2.2 Process Equipment and Catalysts

Conventional methanol production processes based on steam methane reforming or coal gasification use CO hydrogenation. These processes first produce syngas, a mixture of CO and H<sub>2</sub>. Therefore, when designing the green methanol synthesis process with CO<sub>2</sub> instead of CO, parts of the production process must be updated to accommodate CO<sub>2</sub>. The catalyst type, specific temperature, and pressure must be considered. Moreover, as CO<sub>2</sub> hydrogenation produces water, water management and tolerance of the materials used must be carefully chosen (Marques et al., 2024).

The CO<sub>2</sub> hydrogenation process generally operates at 200-300 °C and 50-100 bar (Marques et al., 2024). The trade-off in reaction temperature is that higher temperatures in the process enhance the CO<sub>2</sub> conversion rate but reduce the CO<sub>2</sub> selectivity. Furthermore, to avoid weakening the process due to its byproduct H<sub>2</sub>O, strategies such as hydrophobic catalyst surfaces, water-separating membranes, and dehydrating agents can be used.

Efforts to develop catalysts for CO<sub>2</sub> hydrogenation are currently ongoing, and Marques et al. (2024) argue that there are no fully developed catalysts on a commercial scale that are used today in the production of e-methanol. On the other hand, Agyekum et al. (2025) argue that similar catalysts can be used for CO<sub>2</sub> hydrogenation as in CO hydrogenation. The switch from CO to CO<sub>2</sub> may reduce overall catalyst activity and stability of the catalysts. Impurities such as sulfur deactivate Cu based catalysts (Prašnikar and Likozar, 2022). Generally, less than 0.1 ppm should be aimed for. Furthermore, oxygen impurities cause the catalyst to oxidize, further deactivating it (Ruland, 2020).

The most popular e-methanol synthesis method is heterogeneous catalytic conversion (Marques et al., 2024). In this process, solid catalysts are used for CO<sub>2</sub> conversion to MeOH. The authors suggest that it is efficient and can be scaled up for industrial use. Industrial processes predominantly use catalysts such as copper, zinc oxide, and aluminum oxide (Cu/ZnO/Al<sub>2</sub>O<sub>3</sub>). For the separate RWGS reactor, Choi et al. (2024) suggest that noble metals, such as Pt, Pd, Rh, Au, Ru, and Ir, are currently predominantly used. These noble metals have excellent H<sub>2</sub> dissociation abilities.

However, excessive dissociation and strong CO adsorption can inhibit the release of CO, which can facilitate the production of CH<sub>4</sub> instead of CH<sub>3</sub>OH. Therefore, cost-effective transition metals such as Cu, Fe, Ni, and Co are being investigated as possible RWGS catalysts. Especially Cu is abundant and an already widely applied catalyst, making it an attractive option (Choi et al., 2024).

## 4.3 Market Outlook

This section analyzes the current market as well as reviews the estimates for future methanol markets and the drivers globally.

### 4.3.1 Methanol Supply and Demand

The applications of methanol as a chemical feedstock and fuel have increased significantly and expanded its demand in recent decades. The demand has increased from 51.7 Mt per year in 2011 to 98 Mt per year in 2020 (IRENA, 2021), which is almost a 100 % increase. The global demand in 2050 is estimated to reach 500 Mt per year if current trends continue. The sharp increase in demand for chemicals in China may be a reason for the dramatic surge in global demand for methanol. In 2011, China consumed 27 % of global methanol, while North America and Western Europe accounted for 7 % and 6 %, respectively (Tabibian et al., 2023).

Table 2 shows the distribution of methanol demand and supply globally based on 2024 values (Methanex, 2025a). As the table shows, China's methanol demand had increased to 60 % in 2024, while the demands of North and Latin America, and Europe total only 20 %. For production, China and Middle Eastern countries dominate, with 45 % and 25 % respectively. While China is also a high consumer, the Middle East focuses on exports.

**Table 2:** Regional distribution of global methanol production and demand (Methanex, 2025a).

<b>Region</b>	<b>Production share (%)</b>	<b>Demand share (%)</b>	<b>Comment</b>
Europe (incl. Russia)	5	10	Approximately 65% of production is in Russia
North America / Latin America	20	10	Major production hubs along the U.S. Gulf Coast and in Trinidad
Middle East / Africa	25	5	Around 75% of production from Iran (~45%) and Saudi Arabia (~30%)
China	45	60	Roughly 85% of production based on coal feedstock
Asia Pacific	5	15	Production mainly located in New Zealand and Malaysia

Methanol’s primary use is as a feedstock within the chemical industry today. It is used to produce various everyday chemicals that are used to create products such as fleece, paints, adhesives, vehicle parts, medical equipment, and plastics. Currently, two-thirds of global methanol production is used by the chemical industry, and one-third is used in industrial boilers, transport, and cooking (IRENA, 2021).

With increasing decarbonization efforts, methanol has gained attention as a potential alternative to gasoline, diesel, and marine gas oil (MGO) in the future, especially in marine and aviation fuels (IRENA, 2021; Methanex, 2025a). It can be used in internal combustion engines, hybrid and fuel cell vehicles, and vessels (Tabibian et al., 2023). Methanol can be used as a standalone fuel and in fuel blends or as a feedstock for biodiesel production (IRENA, 2021).

Methanol has been used as a fuel additive in various applications globally. A mixture of gasoline and methanol of a 9:1 ratio has been shown to increase mileage and reduce emissions compared to 100 % gasoline. Despite these findings, the extent of methanol incorporation into gasoline blends has been limited. Tabibian et al. (2023) suggest that this is due to opposition from the oil business.

The technological readiness of the components needed to use methanol as a fuel has reached a mature stage. However, the components have yet to be integrated into a system for commercial methanol handling. However, Tabibian et al. (2023) argue that developing methanol-burning engines is achievable for new systems as well as for converting old motor systems. For example, Wärtsilä already offers various methanol engines with cylinder outputs ranging from 200-1350 kW (Wärtsilä, 2023).

However, some studies indicate that other transport alternatives are more suitable than methanol blends. Tabibian et al. (2023) argue that ethanol could be more efficient as a gasoline blend. Ethanol is a more effective additive as it contains around two-thirds of the energy content of gasoline, while methanol contains around half of the energy content of gasoline.

Heavy transport is undergoing a fuel transition, which is expected to increase methanol demand within the sector. Due to the initiatives of the International Maritime Organization (IMO), the IMO2020 law forces ship owners globally to use cleaner fuels (IMO, 2023). The law mandates that greenhouse gas emissions must be reduced by 50 % by 2050 compared to 2008. However, the implementation of IMO2020 has been postponed by one year (IMO, 2025). The directive was originally scheduled to start in March 2027, but since the implementation was delayed, the future of alternative fuels is uncertain.

The most feasible alternative fuels are LNG, methanol, and ammonia. Methanol has some advantages, as it is biodegradable, and it causes less damage to aquatic life in the case of leakage into the sea (Tabibian et al., 2023). However, Barone et al. (2025) note that fossil LNG has less global warming potential than fossil methanol when used as a marine fuel. In their dynamic simulations for sea traffic, LNG showed 10.4 % less CO<sub>2</sub> emissions than methanol for similar shipping paths. This indicates that to minimize emissions, it is vital to differentiate between renewable and fossil transportation fuels prior to their implementation into the system.

#### **4.3.2 Cost of Methanol**

The cost of producing methanol with fossil fuels is in the range of USD 100-250 per tonne today, while the market price of methanol ranges between USD 200-400 per tonne (IRENA, 2021). The estimated cost of producing e-methanol is up to sixteen times higher than that of fossil methanol, posing a significant challenge to its competitiveness. The current prices for e-methanol are estimated at USD 800-1600 per tonne, if CO<sub>2</sub> is sourced from bioenergy with carbon capture (BECC) (IRENA, 2021). However, IRENA (2021) estimates that e-methanol prices could fall to USD 250-630 per tonne by 2050, due to decreasing renewable energy and electrolyzer costs.

The main issue in e-methanol competitiveness is the energy intensity of electrolysis. Currently, producing one tonne of H<sub>2</sub> requires approximately 50 MWh of electricity (e.g., Aminaho et al., 2025). This leads to the price of hydrogen, therefore the price of e-methanol, being susceptible to the local electricity prices. Water electrolysis is estimated to account for 65 % of the total cost of e-methanol production (Sollai et al., 2023). Furthermore, the price is increased by hydrogen having a low volumetric energy density and requiring special handling, storage, transport, and equipment (IRENA, 2021). The price of CO<sub>2</sub> is less significant, estimated at USD 10-50/tCO<sub>2</sub> for BECC technology from flue gas (IRENA, 2021). However, DAC has much higher potential CO<sub>2</sub> costs, estimated to range USD 300-600/tCO<sub>2</sub>.

A techno-economic review on the cost of e-methanol production by Sillman et al.

(2025) concludes that the power-to-methanol process could be profitable if power prices are low enough, CO<sub>2</sub> taxes are high enough, or fossil methanol prices are approximately doubled. The methanol market price is currently approximately 500 €/tMeOH (Methanex, 2025b). Moreover, the competitiveness of e-methanol increases if the price of fossil methanol increases. Currently, the market price of methanol is expected to increase partly as a result of the rapid growth in demand (Methanex, 2025a).

In comparison, estimations for the costs of e-ammonia production today range between USD 410-1240/tonne (Souissi, 2024). The estimated costs for 2050 could range between USD 200-480/tonne, suggests Souissi (2024), or even under USD 400/tonne by 2040 (Cesaro et al., 2021). For e-gasoline and e-diesel, the estimated costs are significantly higher. Ravi et al. (2023) suggest that the levelized costs of production would be USD 4380/tonne and USD 3480/tonne, for e-gasoline and e-diesel, respectively.

### **4.3.3 Methanol Production Incentives**

The European Union has set a binding target of 42.5 % of renewable energy sources in its energy mix by 2030. Within the Renewable Energy Directive, hydrogen is seen as a cornerstone in decarbonizing hard-to-abate sectors (European Commission, 2025). Renewable fuels of non-biological origin (RFNBOs) are fuels based on 100 % renewable hydrogen and biogenic carbon dioxide that have separate targets within the directive. The goal is that by 2030, RFNBOs should at a minimum account 1 % of energy supplied to the transport sector. By 2030, 42 % of the hydrogen supply should be used in RFNBOs, and by 2030, the share should be 60 %.

E-methanol qualifies, therefore, as an RFNBO if it is produced by 100 % renewable H<sub>2</sub> through electrolysis and captured CO<sub>2</sub> from biogenic sources or DAC. However, the renewable energy used in the production of the fuels has distinct rules. The renewable energy used in the production of the RFNBO must be in direct contact with the production facility. Moreover, the energy plant must not have started production more than 36 months before the RFNBO facility (European Commission, 2023). Furthermore, the plant cannot use grid-powered electricity, even if connected to the grid.

However, there are some exceptions for using grid electricity in RFNBO production. In the act, these are referred to as conditions for additionality and rules for temporal and geographical correlation. Grid electricity is accepted through, for example, a power purchase agreement if the energy plant is not older than 36 months before, and the RFNBO plant does not consume more electricity than produced by the electricity provider. To comply with temporal correlation, the electricity consumed must have been produced within one month of consumption until the end of 2029, whereafter the condition is hourly. Meaning that the produced electricity must be consumed by the RFNBO plant within the same hour. The geographical conditions require that the electrolyzer and energy source must be located within the same bidding zone. (European Commission, 2023)

Some exceptions are considered for the conditions under which renewable energy is used. If the energy mix of the bidding zone was 90 % renewables during the previous year, or its emission intensity was below 18 gCO<sub>2</sub>eq/MJ, no additional renewable plant must be built for RFNBO production. Finally, grid connection is accepted if the RFNBO producer can prove that it improves grid stability. If some of the fuel is produced with sources other than those that meet the conditions, that part of fuel production is not considered an RFNBO (European Commission, 2023).

## 5 Materials and Methods

In this section, the research methods and materials used for this thesis are presented. The main assumptions, inputs, and formulas used for the process models and economic analysis are described.

### 5.1 Process Simulation

For a techno-economic analysis, a process simulation of the proposed system is crucial to achieve reliable results. Energy simulation is a powerful tool when scrutinizing a large and complex energy system process. Such investments would be highly risky to execute experimentally or highly time-consuming to perform by hand. Energy simulation enables low-cost predictions on potential behavior and costs. Furthermore, it offers a comprehensive understanding of a process and its associated costs before investment.

The scope of this work focuses on the process modeling of a PEM electrolyzer and methanol synthesis process, and an economic analysis. The simulations include the PEM electrolyzer for oxygen and hydrogen production, as well as the CO<sub>2</sub> hydrogenation process for e-methanol production. The process model scope is shown in Figure 8. As can be seen, the process scope includes inputs and outputs from the oxyfuel boiler, but does not consider the boiler in technical or economic analysis. The results of the technical analysis are used to determine the cost factors for the financial analysis.

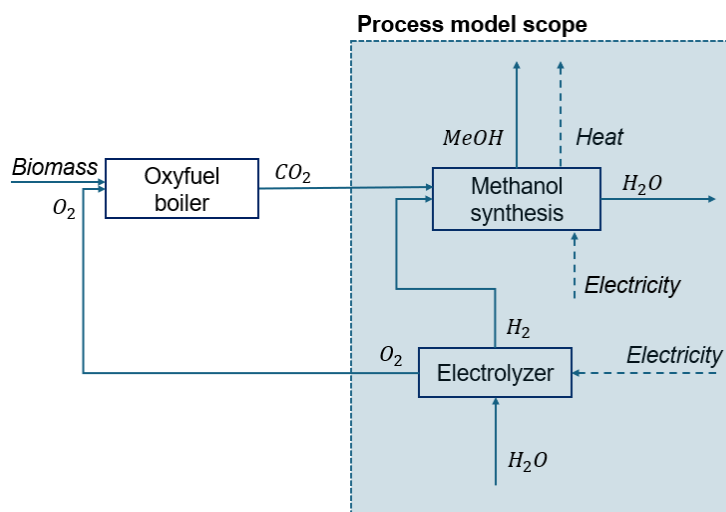


**Figure 8:** Process Model Scope.

For the techno-economic evaluation, process simulation on Aspen Plus™ version 14 is carried out to design the system's sizing, regarding energy and mass requirements to achieve an optimized methanol production system. Aspen Plus is a process

modeling tool formed by a joint research project between Massachusetts Institute of Technology (MIT) and U.S Department of Energy called Advanced System for Process Engineering (ASPEN). It allows for building and simulating chemical processes using complex calculations to optimize and predict performance. The software uses complex calculations to model mass and energy balances and streams for different processes. Aspen Plus is used in processes such as refining, petrochemicals, and pharmaceuticals.

This thesis is a system-level analysis of a comprehensive process; detailed modeling, such as kinetic reaction models, is omitted. This is a limitation, as this analysis does not consider process details that would make the results more realistic. However, the system-level approach allows for an initial thermodynamic review of the technology and its associated lifetime costs.

### 5.1.1 Electrolyzer

A PEM electrolyzer was chosen to produce hydrogen for the methanol production system. The benefits of the PEM system are its compact and simple system design, fast response time, high efficiency, and current density, and the ability to provide high-purity hydrogen. This electrolyzer is especially recommended for its insensitivity to power supply fluctuations and intermittency associated with renewable electricity sources (Barbir, 2005). Therefore, PEM is considered the most plausible option for hydrogen produced with a fluctuating power supply, which is assumed to be the case in this methanol synthesis system.

The model was created to simulate a real-life electrolyzer, similar to models by Zaccara et al. (2020) and Pratama et al. (2023), by combining various simulation blocks. Figure 9 shows the created Aspen model of the electrolyzer, where each block represents different functions. The reactor RSTOIC and separator SEP1 represent the electrolyzer stack, the H2RICH stream and its separators represent the cathode, and the O2RICH stream represents the anode.

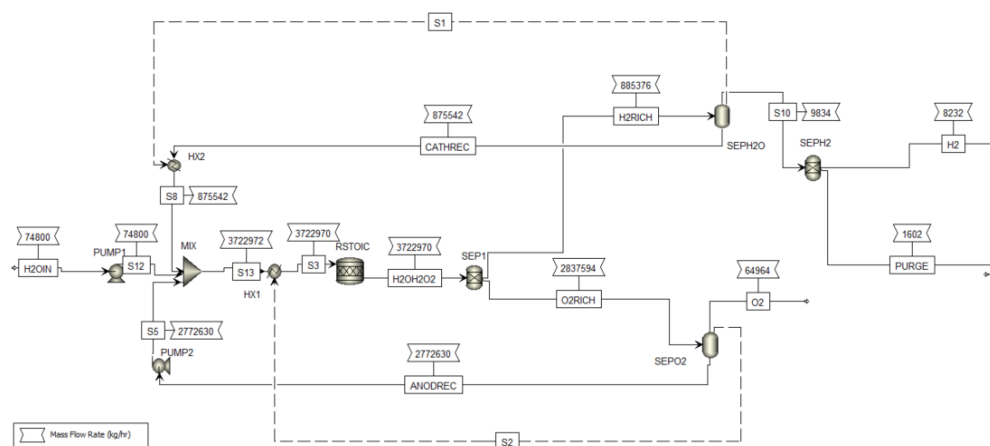


**Figure 9:** PEM Electrolyzer Model in Aspen Plus.

The water-splitting reaction, as in Equation 1, is modeled stoichiometrically with the RSTOIC reactor. The outgoing stream is divided into a hydrogen-rich cathode stream and an oxygen-rich anode stream, which is modeled with the separator SEP1. The reactor is modeled at a pressure of 15 bar and a temperature of 70 °C. The cathode pressure remains at 15 bar, while the anode is depressurized to 1.5 bar (Zaccara et al., 2020). The single-pass H<sub>2</sub>O conversion in the reactor is assumed to be 0.05. For the system to achieve a higher conversion rate, the passing water is recycled back into the reactor both from the cathode and anode with streams CATHREC and ANODREC.

The model includes several gas cleaning blocks to achieve high-purity gases. Due to electro-osmotic drag, for every mole of H<sub>2</sub> leaving the membrane, 5 moles of ceH<sub>2</sub>O are assumed to cross over to the cathode side from the anode side (Friedrichs-Schucht et al., 2024). Similarly, some hydrogen crosses over to the anode and oxygen to the cathode. As in Barbir (2005), the permeation of hydrogen to the anode side and oxygen to the cathode side is calculated as:

$$J_{\text{H}_2,\text{perm}} = (0.0009 e^{0.025T}) \Delta P \quad (5)$$

Oxygen permeation is considered to be 50 % of the hydrogen permeation (Rivera-Tinoco et al., 2016). Equation 5 gives a hydrogen permeation of 0.33 % to the anode side and oxygen permeation of 0.17 % to the cathode side. The water, hydrogen, and oxygen crossover is considered in the input of the SEP1 separator to realistically model the flow compositions of the anode and cathode streams. The hydrogen-rich stream at the cathode side is then flashed from water completely in block SEPH<sub>2</sub>O. The hydrogen is further purified in a membrane downstream, which is represented by block SEPH<sub>2</sub>. The oxygen stream requires only a single separation stage to achieve high-purity oxygen in separator SEPO<sub>2</sub>.

As the Aspen model does not consider power inefficiencies for the electrolyzer, the final required electrical capacity of the electrolyzer was calculated by considering a 70 % power efficiency with the final results (e.g., Aminaho et al., 2025; Şahin, 2024).

### 5.1.2 E-methanol CO<sub>2</sub> Hydrogenation

The required capacities of the simulated methanol synthesis plant and electrolyzer were calculated based on the CO<sub>2</sub> mass flow of the case study plant to maximize the CO<sub>2</sub> utilization rate. The required capacity is assumed according to stoichiometry. The molar ratio of H<sub>2</sub> and CO<sub>2</sub> required in the synthesis is 3:1 of CO<sub>2</sub>:H<sub>2</sub>. The molar mass of CO<sub>2</sub> is 44.06 g/mol and of H<sub>2</sub> 2.02 g/mol. Therefore, to create methanol, every 44.06 g of CO<sub>2</sub> requires 6.048 g of H<sub>2</sub>. The initial input values for the model are presented in Table 3.

The simplified methanol production system is shown in Figure 10. The main inputs in the methanol synthesis process are CO<sub>2</sub> and H<sub>2</sub>. CO<sub>2</sub> is assumed to be stored in liquid phase in storage tanks at 17 bar and -17 °C before being fed into the methanol synthesis plant. The CO<sub>2</sub> input stream is heated to the gas phase and compressed

**Table 3:** Process input data.

Parameter	Value	Unit
CO <sub>2</sub> input	59.6	tCO <sub>2</sub> /h
H <sub>2</sub> input	8.2	tH <sub>2</sub> /h

before being mixed with the hydrogen and recycled gas streams. The hydrogen input stream is assumed to be fed directly from the electrolyzer at 15 bar and 70 °C. The hydrogen is compressed and mixed with CO<sub>2</sub> and recycled gases before entering the reactor.

The reactor block chosen for the simulation is the RSTOIC, a simple model that lets the user simulate the reactor by specifying the reactor stoichiometry and conversions. The reactions are modeled as instantaneous, omitting kinetic modeling. Kinetic modeling for CO<sub>2</sub> hydrogenation has been thoroughly described by, for instance, Leonzio (2019) and Van-Dal (2013). The reactor is modeled with reactions in Equations 2, 3, and 4.

The product leaving the reactor is a mixture of methanol, water, and unreacted gases. These are separated in FLASH1 by decreasing the temperature to 35 °C. The unreacted gases are separated and recycled back into the reactor by stream S2. To avoid accumulation of inert and byproducts in the reactor, a minimum of 2 % of the unreacted gas stream is purged. The stream leaving FLASH1 is depressurized to atmospheric pressure in VLV for further separation of unreacted gases and the methanol-water mixture. The unreacted gases are fed into the recycle stream to re-enter the reactor. The methanol mixture continues to the distillation column DISTIL, where water and methanol are separated.

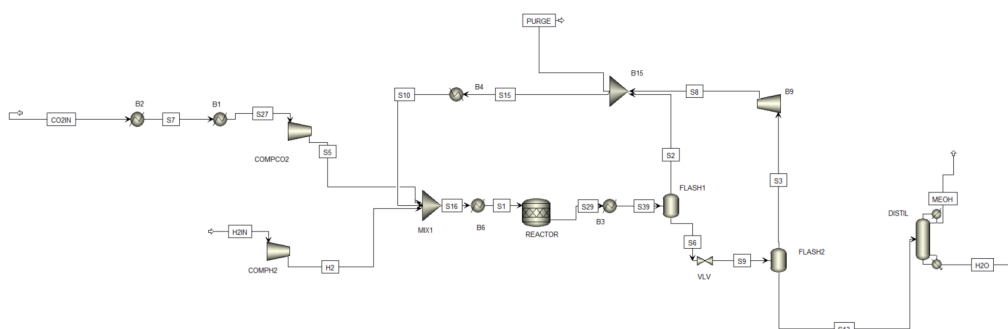


**Figure 10:** The First MeOH Synthesis Model.

### 5.1.3 Heat Recovery and Process Integration

The heating and cooling systems of the methanol production and electrolysis processes were assessed to identify potential synergies. As both systems are exothermic, it poses the possibility to integrate the heat streams within the process or alternatively sell the

heat to, for instance, the district heating network.

Heat integration opportunities were first assessed with the Aspen Plus Energy Analyzer, which gives an estimation of the streams that are possible to integrate. Furthermore, streams in need of cooling and streams in need of heating were assessed and compared in a pinch analysis to identify potential synergies. Heat that can not be integrated within the processes is assumed to be fed into the district heating network. Heat integration was realized by adding heat exchangers and circulating district heating water as the heat transfer medium, as shown in Figure 11. The carbon dioxide stream is presented in burgundy, hydrogen in green, water streams in blue, and the methanol stream in red.

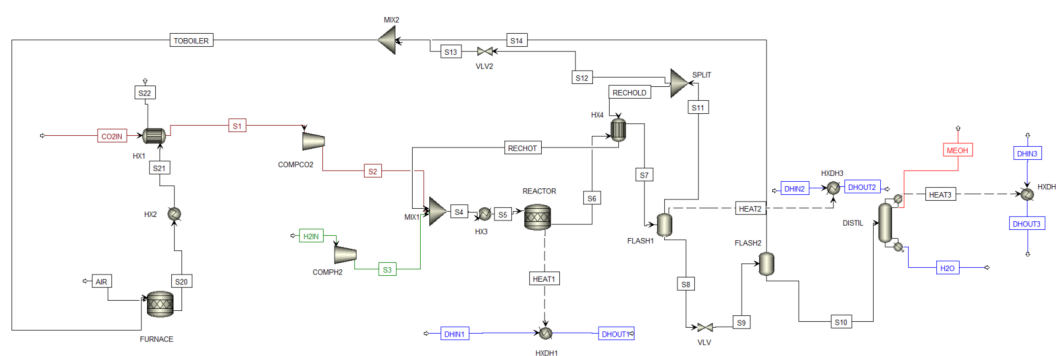


**Figure 11:** Heat Integrated Methanol Synthesis Model

The electrolyzer and methanol synthesis system produces excess heat, which was both integrated in the process and assumed to be sold. All of the possible heat integration solutions were purposely not utilized to avoid risks. An excessively thorough heat integration leads to a larger possibility of one fault within the process to enormously impact another process function. The units were modeled sufficiently independently of each other so that an outage in one unit would not cause the issue to cascade upstream and further intensify the problem in the process.

The heat from the reactor is recycled into the process, and all other excess heat is assumed to be sold to the district heating network or cooled by cooling towers. The product leaving the reactor is separated from unreacted gases in FLASH1, which requires a decreased temperature. The temperature is changed in the gas-gas heat exchanger HX4, which decreases the temperature of the product leaving the reactor and increases the temperature of the recycle stream RECHOT to a temperature as close as possible to the required reactor temperature.

The heat from the reactor, FLASH1, and the distillation column is fed into the district heating network. The amount of district heating water required for the methanol synthesis process was determined to ensure that the inlet and outlet water temperatures meet the requirements in Table 4. Meaning that the mass flow was determined so that the inlet water at 65 °C is heated to 85 °C, which is then circulated back into the district heating network. The assumed heating and cooling water temperatures are

shown in Table 4.

**Table 4:** Cooling and heating water inlet and outlet temperatures.

Stream	Inlet Temperature (°C)	Outlet Temperature (°C)
Cooling water	20	40
Heating water	65	85

The available energy fed into the district heating network was then calculated with Equation 6.

$$Q_{DH} = c_{\text{water}} \dot{m} \Delta T \quad (6)$$

where  $Q_{DH}$  is the heat delivered to the district heating network,  $c_{\text{water}}$  is the specific heat capacity of water:  $4.18 \text{ kJ kg}^{-1} \text{ K}^{-1}$ ,  $\dot{m}$  is the mass flow,  $\Delta T$  temperature difference of the water between outlet and inlet at consumption. The  $\Delta T$  is conservatively assumed to be 20 K.

The available excess heat from the PEM electrolyzer was estimated based on (Kumar et al., 2025) and scaled according to the PEM electrolyzer size in this study.

#### 5.1.4 Efficiencies

The carbon utilization rate used in this case study was 100 %, meaning that the sizing of the plant was carried out so that the  $\text{CO}_2$  produced by the oxyfuel boiler is fully used. By maximizing the use of  $\text{CO}_2$ , the amount of harmful GHG intentionally vented out into the atmosphere is minimized. Based on the main assumption of the  $\text{CO}_2$  utilization rate, the other key performance indicators (KPIs) evaluated in this thesis are the power-to-methanol efficiency,  $\text{CO}_2$  conversion,  $\text{CO}_2$ -to-methanol efficiency, hydrogen efficiency, and methanol yield.

The power-to-methanol efficiency, as defined in Equation 7 is the ratio of methanol energy output to the total electricity capacity in the electrolyzer and synthesis process. The lower heating value (LHV) used is 19.9 MJ/kg (Methanol Institute, 2016).

$$\eta_{\text{PtMeOH}} = \frac{\dot{m}_{\text{MeOH}} \text{LHV}_{\text{MeOH}}}{P_{\text{el}}} \quad (7)$$

The  $\text{CO}_2$  conversion in Equation 8 describes the amount of carbon dioxide that undergoes a reaction during the process. This KPI gives an indication of how much  $\text{CO}_2$  emissions are avoided by the process.

$$\eta_{\text{CO}_2} = \frac{\dot{m}_{\text{CO}_2, \text{in}} - \dot{m}_{\text{CO}_2, \text{out}}}{\dot{m}_{\text{CO}_2, \text{in}}} \quad (8)$$

To further evaluate the amount of  $\text{CO}_2$  that has been converted to a valuable product, in this case MeOH, Equation 9 was used.

$$\eta_{\text{CO}_2 \rightarrow \text{MeOH}} = \frac{\dot{m}_{\text{MeOH}}}{\dot{m}_{\text{CO}_2, \text{in}}} \quad (9)$$

The hydrogen efficiency in Equation 10 describes the ratio of reacted hydrogen during the process.

$$\eta_{\text{H}_2} = \frac{\dot{m}_{\text{H}_2, \text{in}} - \dot{m}_{\text{H}_2, \text{out}}}{\dot{m}_{\text{H}_2, \text{in}}} \quad (10)$$

Finally, the methanol yield was computed with Equation 11. It gives the ratio between the produced MeOH and the input CO<sub>2</sub> and describes how much valuable product can be attained per unit of CO<sub>2</sub>.

$$Y_{\text{MeOH}} = \frac{\dot{m}_{\text{MeOH}}}{\dot{m}_{\text{CO}_2, \text{in}}} \quad (11)$$

## 5.2 Economic Analysis

A techno-economic analysis was conducted to estimate the profitability of e-methanol production. Costs for the methanol and electrolysis plants are obtained from available literature. Capital costs, fixed operating costs, and variable operating costs are sufficient to evaluate the profitability of this e-methanol production case. Table 5 shows the main assumptions for the feasibility analysis.

**Table 5:** Economic parameters used in the techno-economic assessment.

Parameter	Value
Operational lifetime	25 years
Annual operating hours	8 000 h
Real discount rate	5.9 %
Reference year	2024

### 5.2.1 Capital Expenditures

The bare equipment costs were estimated individually for each process component, such as the flash drums, heat exchangers, compressors, and reactors, using a scaling relation adapted from, for instance, Gelten et al. (2026); Nyári et al. (2020). For each equipment item  $i$ , the cost was determined according to Equation (12):

$$\text{PEC}_{\text{model},i} = \text{PEC}_{\text{lit},i} \left( \frac{Q_{\text{model},i}}{Q_{\text{lit},i}} \right)^M \quad (12)$$

where  $\text{PEC}_{\text{model},i}$  is the purchased equipment cost of component  $i$  estimated in this work,  $\text{PEC}_{\text{lit},i}$  is the corresponding reference cost from literature,  $Q_{\text{model},i}$  and  $Q_{\text{lit},i}$  are

the equipment sizes or capacities in this study and in the literature source, respectively, and  $M$  is the cost-scaling exponent. In this work, a value of  $M = 0.6$  was applied (Nyári et al., 2020). The total PEC of the plant was then obtained by summing over all individual components as

$$PEC_{\text{total}} = \sum_i PEC_{\text{model},i}. \quad (13)$$

Furthermore, CAPEX also considers installation, construction, start-up, working capital, as well as research and development costs. The CAPEX for the methanol synthesis plant was estimated with a simplified relation between PEC and CAPEX based on (Collodi et al., 2017) in Equation 14:

$$CAPEX = 6.32 \cdot PEC_{\text{total}} \quad (14)$$

**Table 6:** Purchased equipment costs of the MeOH plant scaled from Ong et al. (2024).

Unit	Name	Cost (€/unit)
Compressor	COMPCO2	7 188 260.68
	COMPH2	17 766 833.92
Reactor	REACTOR	353 690.64
Furnace	FURNACE	3 263 628.05
Flash	FLASH1	273 972.31
	FLASH2	448 661.63
Distillation column	Tower	1 712 893.70
	Condenser	588 374.18
	Reboiler	984 496.66
Heat exchanger	HX1	218 417.74
	HX2	182 329.31
	HX3	1 680 407.69
	HX4	594 218.47
Cooler	HXDH1	955 022.11
	HXDH2	2 751 753.45
	HXDH3	1 085 212.93

All purchased equipment costs were reported for the year 2025. Values originating from prior years were adjusted

$$PEC_{2025} = PEC_0 \left( \frac{I_{2025}}{I_0} \right) \quad (15)$$

where  $PEC_{2024}$  is the cost updated to 2024,  $PEC_0$  is the original reported cost,  $I_0$  is the value for the original reference year, and  $I_{2024}$  is the value for 2024.

## 5.2.2 Operational Expenditures

The operational expenses (OPEX) of the plant are considered as annual expenses related to the plant's activity. The OPEX was separated into fixed and variable OPEX, depending on whether they are dependent on the output of the plants. Fixed OPEX occur regardless of plant activity, therefore, it includes costs such as operating labor, routine maintenance, and overhead costs such as insurance, property taxes and fees, and research and development (Spoof-Tuomi and Manfo, 2025). Following Spoof-Tuomi and Manfo (2025), the deionized water cost is not separately estimated, but assumed to fall within the fixed OPEX. The fixed OPEX can therefore be estimated according to Equation 16.

$$OPEX_{\text{fixed},i} = 0.02 \cdot CAPEX_i \quad (16)$$

where  $i$  denotes the type of investment; electrolyzer or methanol plant.

Variable OPEX includes costs that vary with the rate of production, such as utility, feedstock, and operating labor costs. The primary raw materials for the process were considered as  $CO_2$ ,  $H_2$ , and electricity. The  $H_2$  stream in the methanol plant is considered at zero cost. However, instead of considering the cost of the  $H_2$  stream, the total cost of the PEM electrolyzer is considered.

$$OPEX_{\text{variable},i} = C_{\text{electricity}} \cdot E_{\text{consumed},i} + C_{\text{utilities},i} + C_{\text{replacement},i} \quad (17)$$

Where  $C_{\text{electricity}}$  is the cost of electricity,  $E_{\text{consumed}}$  is the electricity consumption of plant  $i$ ,  $C_{\text{utilities}}$  the lump sum cost of utilities received from Aspen Plus, and  $C_{\text{replacement}}$  is the replacement cost associated with plant  $i$ . In this study, meaning the replacement of the electrolyzer stack or methanol synthesis catalyst.

Electricity costs can be estimated according to recent grid prices or the LCOE of existing wind and solar power plants. However, the profitability of separate wind and solar power plants varies according to the selected location. Furthermore, the operating hours of an independent renewable energy source are volatile due to fluctuating weather conditions. Therefore, the electricity price for the base case analysis was chosen assuming that the methanol plant is connected to an independent plant and the grid (Eurostat, 2025; IRENA, 2025). This way, the plant receives electricity from the grid when renewables are not generating power. The estimated realized electricity cost and other main assumptions used to calculate the OPEX are shown in Table 7. The electricity price is assumed to include energy tax, capacity costs, and energy costs.

**Table 7:** Summary of variable OPEX assumptions for the electrolysis and methanol plants.

Category	Comment	Value	Unit
Electricity price	Estimated from Eurostat (2025) and IRENA (2025)	50	€/MWh
CO <sub>2</sub> price	Estimate of carbon capture price	20	€/tCO <sub>2</sub>
Cooling water price	Ong et al. (2024)	1.10	€/MWh
Methanol synthesis catalyst	Replaced every 3 years (Nyári et al., 2020)	8.8	€/kg
Decommissioning	Assumed net zero due to salvage value (Collodi et al., 2017)	0	–

### 5.2.3 Levelized Cost of Methanol

To estimate the cost of producing e-methanol, the method of levelized cost was used, according to Equation 18.

$$\text{LCOM} = \frac{\sum_{t=0}^N \frac{C_{\text{total},t}}{(1+r)^t}}{\sum_{t=0}^N \frac{Q_{\text{MeOH},t}}{(1+r)^t}} \quad (18)$$

Where  $C_{\text{total},t}$  is the total annual cost in year  $t$ , including the fixed and variable operating expenses of both the methanol plant and the electrolyzer, as well as the replacement costs for the catalyst or electrolyzer stack.  $Q_{\text{MeOH},t}$  is the methanol production in year  $t$ ,  $r$  is the discount rate, and  $N$  is the plant lifetime in years.

The levelized cost of methanol is considered first hand as €/tonne, but is converted to energy-based units for it to be comparable with currently used marine fuel alternatives.

**Table 8:** Assumptions used for converting fuel costs to energy units.

Parameter	Value	Unit	Source
<b>Methanol</b>			
LHV of methanol	19.9	MJ/kg	Methanol Institute (2016)
Energy per tonne of methanol	5528	kWh/t	
<b>Marine Gas Oil</b>			
LHV of MGO	43	MJ/kg	Aronietis et al. (2016)
Energy per tonne of MGO	11 944	kWh/t	

## 5.3 Sensitivity Analysis Framework

This section provides an overview of the methodology used in the sensitivity analysis. The varied variables and values are presented.

### 5.3.1 Electrolyzer Cost and Electricity Price

Due to large fluctuations in CAPEX estimations for PEM electrolyzers in literature, a sensitivity analysis on the possible costs for the electrolyzer was conducted. As Table 9 shows, the scenarios are divided into optimistic, base case, and pessimistic cost estimates of 800 €/kW, 1800 €/kW, and 2500 €/kW, respectively.

**Table 9:** PEM electrolyzer CAPEX values used in the sensitivity analysis.

Case	CAPEX (€/kW)	Source
Optimistic	800	Badgett et al. (2024)
Base case	1800	Deloitte (2021); Spoof-Tuomi and Manfo (2025)
Pessimistic	2500	European Hydrogen Observatory (2025a)

Similarly, the levelized cost is analyzed under different electricity prices, as shown in Table 10.

**Table 10:** Electricity price sensitivity cases.

	Base	-30%	+30%	+100%	+150%
Electricity price (€/MWh)	50	35	65	100	125

### 5.3.2 Side Stream Revenues

The potential side-revenue streams from excess oxygen and heat were also scrutinized in the sensitivity analysis. Due to uncertainties in oxygen market prices and demand, their impact on the LCOM was analyzed. Furthermore, the demand for district heating has an impact on the amount of side-stream revenues and cooling needed, which are analyzed in this sensitivity.

The analysis was conducted by examining different levels of annual full-load hours of district heating demand. The compared values are 0, 2000, 4000, 6000, and 8000 hours per year. The methanol synthesis plant is assumed to run for 8000 h/a. If district heating can not be sold, the plant requires cooling, which in turn is an expense instead of a revenue. The cooling expenses were calculated with 1.10 €/MWh based on Ong et al. (2024).

The possible revenues received from selling heat were based on the energy prices of district heating in Finland. The district heating kilowatt-hour price consists of the energy price, demand charge, and energy tax. As the demand charge and energy tax do not affect the possible revenues of selling excess heat, the used value is based on the energy price portion of the full district heating prices in Finland (Energiateollisuus

ry, 2025). The value chosen to use for calculations was 80 €/MWh, as it reflects the average price during high-demand months.

The excess oxygen produced by the electrolyzer was also reviewed as a potential side-stream revenue source. Current market prices for oxygen are approximately 100 €/O<sub>2</sub>/t (Marques et al., 2024). However, with an increasing number of electrolyzers under construction, the oxygen supply is expected to increase significantly, which could negatively impact the oxygen prices. Therefore, a sensitivity analysis was conducted on the impact of the oxygen price on the levelized cost of methanol.

The amount of oxygen sold was based on the difference between the produced oxygen and the oxyfuel boiler demand, which for this case study was 19.8 tO<sub>2</sub>/h. All of the excess oxygen was assumed to be sold. The sensitivity was conducted for the prices 25 €/tO<sub>2</sub>, 50 €/tO<sub>2</sub>, 75€/tO<sub>2</sub>, and 100 €/tO<sub>2</sub>.

### 5.3.3 Renewable Energy Availability

To comply with RFNBO directives, the electrolyzer and methanol plant must use renewable energy sources for their production of hydrogen and methanol (European Union, 2023). Because renewable energy sources are highly volatile and weather-dependent, their availability and intermittency must be considered when planning their use as electricity sources. The volatility impacts, for instance, the capacity, energy production potential, and therefore methanol yield. This sensitivity analysis considers seasonal variation in renewable energy availability to estimate the available power. Furthermore, while the PEM electrolyzer is assumed to ramp up and down with power, the methanol plant is assumed to operate continuously. This study assumes the power source is onshore wind.

Studies suggest that wind speeds are higher during winter and spring months, and lower during summer and autumn months (e.g., Fingrid Oyj, 2025; Jung and Schindler, 2020). This leads to seasonal variation in wind power yield. To conduct the analysis on seasonal variation, data were acquired from Fingrid Oyj (2025). Data on Finnish wind power generation with 15-minute accuracy was used in complement to the total installed wind power capacity during the years 2020-2024. Estimates on the capacity factors for each hour were estimated with Equation 19.

$$CF = \frac{E_{\text{actual}}}{P_{\text{nom}} \cdot T} \quad (19)$$

where  $E_{\text{actual}}$  is the actual energy produced (MWh),  $P_{\text{nom}}$  is the nominal installed capacity (MW), and  $T$  is the time period considered (h).

The required capacity of the plant is assumed to be equal to the electricity demand of the electrolyzer and methanol plant. All electricity produced is then consumed by the plants, leaving no excess power to be sold to the network.

As the methanol production process is assumed to be constant, the required electrolyzer capacity defines the power capacity required from the wind power plant. The methanol

production requires a constant flow of hydrogen at 8.2 tH<sub>2</sub>/h. The actual hydrogen production is assumed to fluctuate with wind power production, requiring hydrogen storage. When there is excess power available, excess hydrogen is produced and sent to storage. When less power is available, the required amount of hydrogen for the methanol process is then complemented by discharging the hydrogen storage. The hydrogen yield from the electrolyzer is estimated by considering the specific electricity consumption per kilogram of hydrogen produced in kWh/kgH<sub>2</sub> according to Equation 20:

$$m_{\text{H}_2} = \frac{E_{\text{el}}}{e_{\text{H}_2}} \quad (20)$$

where  $m_{\text{H}_2}$  is the produced hydrogen mass (kgH<sub>2</sub>),  $E_{\text{el}}$  is the electrical energy supplied by the wind power plant (kWh), and  $e_{\text{H}_2}$  is the specific electricity consumption of hydrogen production (kWh/kgH<sub>2</sub>).

One optimal solution for the electrolyzer capacity was calculated with the Microsoft Excel Goal Seek function. The optimal model assumes that the PEM electrolyzer is able to ramp up and down perfectly with wind power production. Furthermore, the storage inventory must always be larger than 0. The optimization was carried out by looking for the optimal capacity of the electrolyzer to satisfy the annual hydrogen demand of 65.6 ktH<sub>2</sub>, given the available wind power.

### 5.3.4 Carbon Tax and Market Price

The local carbon tax escalation is a crucial factor when evaluating the profitability of e-methanol compared to its fossil alternatives. This sensitivity aims to find the magnitude of the carbon tax that increases fossil methanol market prices of methanol to the same value as e-methanol. Table 11 shows the main assumptions made for the sensitivity analysis.

**Table 11:** Base assumptions for the carbon tax impact on methanol production cost.

Parameter	Value	Source
Emission factor (tCO <sub>2</sub> /tMeOH)	2.19	Hamelinck and Bunse (2022)
Cost of production excluding carbon tax (€/tMeOH)	319	IRENA (2021) and Methanex (2025b)
Carbon tax in December 2025 (€/tCO <sub>2</sub> )	84	International Carbon Action Partnership (2025)

The required minimum carbon tax was estimated by assuming that general production costs remain the same and the market price is adjusted with the additional tax factor. As the majority of fossil methanol is produced with natural gas, the carbon price was estimated using the emission factor of methanol produced with natural gas (Hamelinck and Bunse, 2022). The minimum carbon tax required to match the fossil methanol

price with the e-methanol price was determined using the Microsoft Excel Goal Seek function.

## 6 Results and Discussion

This section presents and interprets the technical and financial results of the process model. The research questions are answered and discussed.

### 6.1 Technical Results

The technical results that are presented are the power consumption, heat and mass balances, and the impact of integrating excess heat streams. These factors give valuable information on the system's viability and profitability, which can be compared to literature and other existing plants.

#### 6.1.1 Energy Requirements

The power consumption of the system was received from the electrolyzer and methanol synthesis models. The final required electrolyzer power capacity is 475 MW, which is mainly because of the electrolyzer stack. The methanol power requirement is 9.6 MW, which is carried out by the compressors. Figure 12 shows the main electricity-consuming components in both the electrolyzer and methanol synthesis. For reference, the case study boiler's electrical output is 55 MW, which is roughly 10 % of the total power capacity needed for the integrated plant.

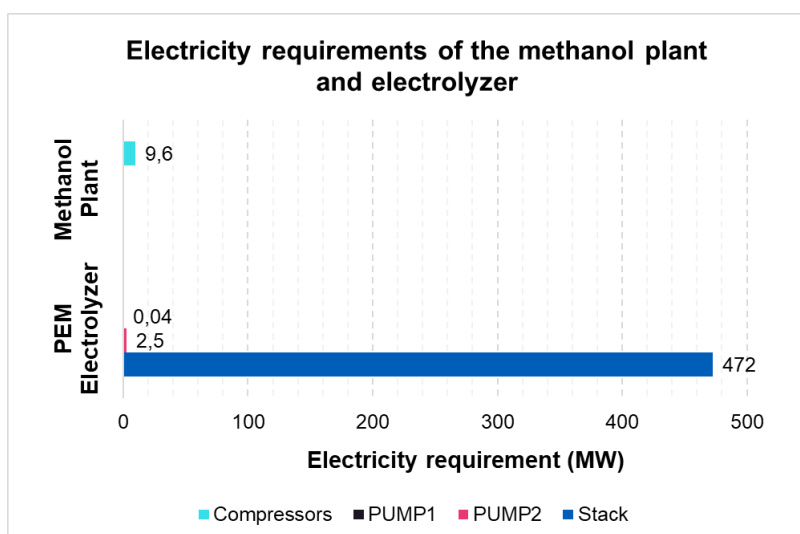


**Figure 12:** Electricity requirements of the electrolyzer and methanol plant.

The recycle and water pumps require marginal power capacity in the system, as the table above shows. The power demand of the final hydrogen purification stage is not provided by the Aspen model. It is assumed to be negligible and has no material impact on the overall uncertainty of the results. The PEM electrolyzer power consumption per kilogram of hydrogen produced is 53.9 kWh/kgH<sub>2</sub>, which is in line with existing studies (e.g., Deloitte, 2021; Spoof-Tuomi and Manfo, 2025). The required power to split water in electrolysis is enormous, overshadowing the power requirements of the

rest of the process. The rest of the components in the models require energy mainly in the form of heat.

The process model results also show that the PEM electrolyzer requires significantly more heat capacity than the methanol synthesis plant, as Figure 13 shows. The methanol synthesis process requires high temperatures to increase the temperature of the flow into the reactor. However, the mass flows in the methanol process are moderate compared to the electrolyzer's, which is further presented in Section 6.1.2. Due to the low single-pass conversion of water in the electrolyzer, the water recycle rate is high, leading to sizeable mass flows in the recycle streams from the cathode and anode back into the stack. Therefore, the heat exchangers require substantial heat capacity to increase the recycled water's temperature to suffice for the electrolysis.

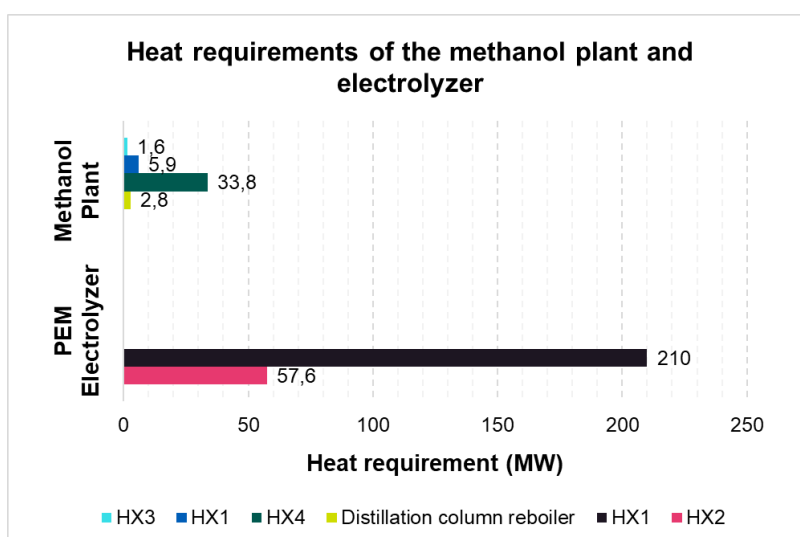


**Figure 13:** Heat requirements in the PEM electrolyzer and methanol plant.

### 6.1.2 Heat and Mass Balances

The integrated methanol production plant produces 37.0 tMeOH/h with a 99.4 % purity. The plant assumes ideal reactant balance, assuming a stoichiometric mix of H<sub>2</sub> and CO<sub>2</sub>. The process stream flows, pressures, and temperatures of the most relevant streams in the methanol synthesis plant are presented in Table 12. Streams S6 and S7 represent the process streams before and after the reactor.

**Table 12:** Stream properties for the methanol plant process streams.

Parameter	H <sub>2</sub> IN	CO <sub>2</sub> IN	S5	S6	Recycle	Purge	H <sub>2</sub> O OUT	MeOH
Mass flow (t/h)	8.2	59.6	333.1	333.1	265.3	7.0	22.0	37.0
Pressure (bar)	15	17	76	76	76	1	1	1
Temperature (°C)	25	-30	210	210	200	29	100	54

The composition of the most relevant streams in the methanol plant are shown in Table 13. As the table shows, the impurities in the product methanol consist of traces of CO<sub>2</sub> and H<sub>2</sub>O. Streams S5 and S6 show the difference in compositions before and after the reaction has occurred.

**Table 13:** Component flow rates in the process streams.

Component (t/h)	H <sub>2</sub> IN	CO <sub>2</sub> IN	S5	S6	Recycle	Purge	H <sub>2</sub> O OUT	MeOH
CO <sub>2</sub>	–	59.6	244.0	190.4	184.4	5.1	–	0.1
H <sub>2</sub>	8.2	–	41.5	34.3	33.4	0.7	–	–
MeOH	–	–	2.2	39.8	2.2	0.2	0.3	36.8
H <sub>2</sub> O	–	–	0.2	22.2	0.2	0.003	21.8	0.1
CO	–	–	45.1	46.4	45.1	0.9	–	–
O <sub>2</sub>	–	–	0.001	0.001	0.001	–	–	–

The results of the PEM electrolyzer are shown separately in the tables below. Table 14 shows the stream properties for the most important streams in the electrolysis process. The electrolyzer produces hydrogen at a rate of 8.2 tH<sub>2</sub>/h at a purity of 99.9 %. The oxygen stream is at 65.5 tO<sub>2</sub>/h at a purity of 99.6 %. All of the hydrogen produced by the PEM electrolyzer is assumed to be fed into the methanol synthesis system. The oxygen is partly fed into the oxyfuel boiler, and the excess is sold as high-purity oxygen or vented into the atmosphere. The oxyfuel boiler requires approximately 45.8 tO<sub>2</sub>/h, resulting in an excess of 19.8 tO<sub>2</sub>/h sold.

**Table 14:** Stream properties for the electrolyzer streams.

Parameter	H <sub>2</sub> O IN	CATHREC	ANODREC	S3	O <sub>2</sub> OUT	H <sub>2</sub> OUT
Mass flow (t/h)	74.8	875.5	2772.6	3723.0	65.6	8.2
Pressure (bar)	1	15	1.5	15	1.5	15
Temperature (°C)	20	20	10	70	10	25

The compositions of the relevant streams in the electrolyzer are shown in Table 15. The recycle streams for H<sub>2</sub>O, CATHREC and ANODREC, are large due to the low single-pass conversion rate in the stack. Similarly, stream S3 entering the stack is significant in size despite the mass flow of the feed-in water being moderate, 74.8 tH<sub>2</sub>O/h. However, both recycle streams are relatively pure, only containing traces of H<sub>2</sub> and O<sub>2</sub>.

**Table 15:** Component mass flows for the electrolyzer streams.

Component (t/h)	H <sub>2</sub> O IN	CATHREC	ANODREC	S3	O <sub>2</sub> OUT	H <sub>2</sub> OUT
H <sub>2</sub>	–	2.0×10 <sup>-4</sup>	3.0×10 <sup>-4</sup>	1.9×10 <sup>-4</sup>	0.003	8.2
H <sub>2</sub> O	74.8	875.6	2772.0	3723.0	0.2	–
O <sub>2</sub>	–	6.0×10 <sup>-4</sup>	1.0×10 <sup>-3</sup>	0.001	65.4	1.0×10 <sup>-3</sup>

One can conclude that the low conversion rate in a single pass through the electrolyzer is a bottleneck in the process, as it results in high recycle mass flows that must later be heated up again. Especially, the anode stream is a high energy consumer, as it requires a low temperature of 10 °C in the flash drum to separate the recycle and oxygen. Moreover, the oxygen brings the majority of the unreacted water to the anode side, leading to higher heating requirements for the recycle from the anode stream. Improvements in conversion rates could therefore reduce water consumption and heating requirements for the electrolysis system.

### 6.1.3 Process Heat Integration

Table 16 shows the heat exchangers modeled within the integrated concept. The heat directly recovered within the process is 33.8 MW in the gas-gas heat exchanger HX4. The heat exchanger transfers energy between the outgoing stream from the reactor and the recycle stream outgoing from the first flash drum FLASH1. The heated recycle stream is fed back into the reactor. The heat exchanger allows the temperature of the stream leaving the separator to increase from 35 °C to 200 °C in the recycle stream. The recycle stream is the only process stream that uses heat directly from within the methanol production system.

The purged stream is also utilized for heat within the process. The purged stream is assumed to enter the oxyfuel boiler, which in turn produces heat for heat exchanger HX1, which increases the temperature of the input liquid CO<sub>2</sub> from -30 °C to 25 °C, which simultaneously results in the CO<sub>2</sub> attaining the gas phase. The heat exchanger HX3 that heats up the stream entering the reactor could utilize the heat from the oxyfuel boiler as well. However, the heat integration for HX3 was not explicitly modeled in this study.

**Table 16:** Heat recovered in internal heat exchangers.

Heat exchanger	Hot stream (°C)	Cold stream (°C)	Heat recovered (MW)
HX4	210 → 115	35 → 200	33.8
HX1	120 → 13	-30 → 13	5.9

In addition to heating the CO<sub>2</sub> and recycle streams, the two streams that require external heating are stream S4 and the distillation column. According to the model, these streams require 1.6 MW and 28.3 MW, respectively. Hence, the integrated process covers 57.0 % of the total heating needs within the process, reducing the external heat demand significantly.

Within the methanol production system, the reactor, the first flash drum FLASH1, and the distillation column DISTIL leave excess heat. The heat is not integrated; it is cooled with assumed circulating district heating water. Table 17 shows the water mass flows for each block and the heat recovered by the water fed. The total cooling need for the system is therefore the sum of the heat recovered, which totals 80.2 MW.

The cooling needs of the process plant can be considered significant, as they are approximately a third of the summertime demand of the city of Helsinki (Helen Oy, 2025). The heating needs of the process are marginal when compared to the cooling needs.

**Table 17:** Water mass flows and heat recovered from process heat sources.

Heat source	Block name	Mass flow (t/h)	Heat recovered (MW)
Reactor	REACTOR	750	19.2
Flash drum	FLASH1	1400	35.0
Distillation column	DISTIL	1100	26.0
PEM Electrolyzer	–	2600	60.5

Furthermore, the PEM electrolyzer produces a large amount of excess heat as well. For the 475 MW electrolyzer in this study, the excess heat produced is estimated at 60.5 MW. This results in the total excess heat produced by the integrated electrolyzer and methanol production plant being 140.7 MW, which must be sold as heat or cooled.

#### 6.1.4 Process Efficiencies

Table 18 reports the key efficiencies of the system and concludes the technical reporting section. All values reported are for the whole integrated system, including the recycles. When considering the LHV of methanol and the total electricity consumed by the electrolysis and methanol production plant, the power efficiency of the produced e-methanol is approximately 42.2 %. The CO<sub>2</sub> conversion in general is 91.3 %, and the percentage of CO<sub>2</sub> that specifically converts to MeOH is 85.4 %. The rest mainly converts into CO due to the RWGS reaction. These results suggest that 8.7 % of the produced carbon dioxide from the oxyfuel boiler leaks into the atmosphere during the synthesis process.

**Table 18:** Summary of key process efficiencies for the integrated methanol plant.

Efficiency metric	Notation	Value (%)
Power-to-methanol efficiency	$\eta_{\text{PtMeOH}}$	42.2
CO <sub>2</sub> conversion	$X_{\text{CO}_2}$	91.3
CO <sub>2</sub> conversion to methanol	$\eta_{\text{CO}_2 \rightarrow \text{MeOH}}$	85.4
H <sub>2</sub> conversion to methanol	$\eta_{\text{H}_2}$	91.5
Methanol yield	$Y_{\text{MeOH}}$	62.1

The H<sub>2</sub> conversion is 91.5 %, where all hydrogen that is not converted is purged. The methanol yield is calculated by considering the mass flow of MeOH relative to the mass flow of CO<sub>2</sub> entering the plant. In this simulation, the yield is 62.1 %. This indicates that minimizing the amount of unreacted gases purged could increase the methanol yield.

## 6.2 Economic Results

The economic results are divided into capital expenditures (CAPEX) and operational expenditures (OPEX), from which the final levelized cost of methanol (LCOM) can be estimated.

### 6.2.1 Capital Expenditures

The total CAPEX considers the initial expenses of the PEM electrolyzer and the methanol synthesis plant. The total CAPEX for the system is estimated at 1 100 M€. As Figure 14 shows, the PEM electrolyzer contributes 855 M€ and the methanol synthesis plant 250 M€ to the total cost. The electrolyzer dominates the costs, contributing 77.1 % of the total capital investment. The high cost of the electrolyzer demonstrates a financial bottleneck in the system, indicating that the feasibility of the e-methanol plant is heavily impacted by the hydrogen production facility price. Therefore, improving the cost efficiency of the electrolyzer could be considered more urgent than developing the cost efficiency of the methanol plant.

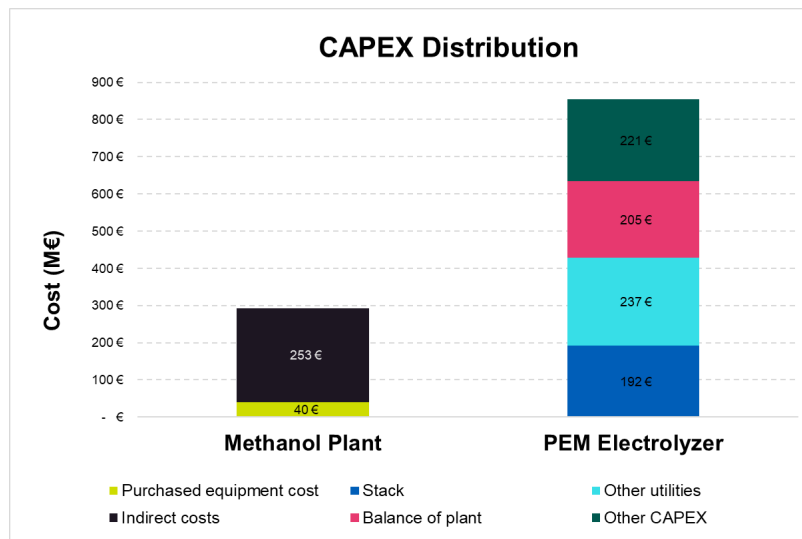


**Figure 14:** Electrolyzer and MeOH Plant CAPEX

Indirect costs dominate the CAPEX of the methanol plant, as shown in the figure above. The equipment cost accounts for only a fraction of the expenses, while the majority of the costs, the indirect costs, are spent on engineering, transportation, installation, and other services. On the other hand, the estimated distribution of the PEM CAPEX is relatively even between the stack, balance of plant (BoP), other utilities, and other CAPEX. The stack costs include equipment, engineering, procurement, and installation. The BoP includes equivalent work regarding other equipment in the electrolyzer, the rectifier, transformer, gas and water separation and feeding systems, and purification. The other utilities include necessary work regarding high voltage transformers, water treatment, cooling, control systems, and other services. Other CAPEX include land and grid fees, insurance, permitting, feasibility study,

contingency, and EPC management (European Hydrogen Observatory, 2025a). No specific factor of the electrolyzer stands out as significantly costly.

### 6.2.2 Operational Expenditures

The total annual OPEX for the combined electrolysis-methanol synthesis plant is estimated at 227 M€. Over the whole lifetime of the system, the total discounted OPEX is estimated at 2 751 M€. As expected, this is larger than the total CAPEX discounted over the project lifetime, mainly due to the high power consumption and cost of the electrolyzer. Figure 15 compares the total annual OPEX for the electrolyzer with the total OPEX of the integrated plant. The electrolyzer is responsible for the overwhelming majority of total operational costs, accounting for 91.3 % of total annual OPEX. This is expected as the methanol synthesis plant operates near autothermal conditions and, due to the high heat integration ratio, does not require much excess heat or power sources.

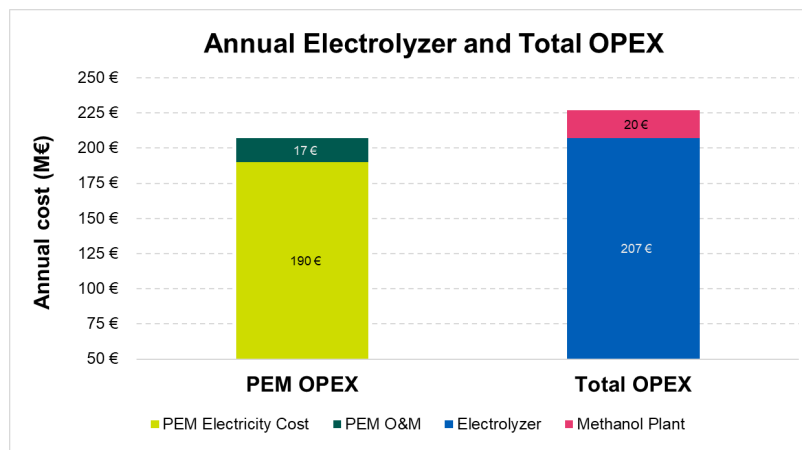


**Figure 15:** Electrolyzer and total system annual OPEX.

The electrolyzer OPEX mainly consists of electricity costs, with only a marginal fraction spent on general operation and maintenance of the PEM electrolysis plant. Water electrolysis is a highly energy-intensive process, leading to high consumption of electricity. As power consumption and price determine the feasibility of clean hydrogen production, local electricity prices are a crucial factor in planning the location of the electrolyzer. Alternatively, when choosing the power source for the electrolyzer, a method with a low levelized cost of electricity should be prioritized. Moreover, improvements in energy efficiency are also highly valuable when aiming to decrease the costs of the electrolyzer.

The OPEX of the methanol synthesis plant is less significant at the system level, but some variation in the contributing variables is evident. Figure 16 shows the breakdown of the variable and fixed annual OPEX of the methanol synthesis plant, excluding all costs of electrolysis. The variable OPEX is significant, exceeding the annual fixed OPEX by more than twice. The variable OPEX consists mainly of the CO<sub>2</sub> associated

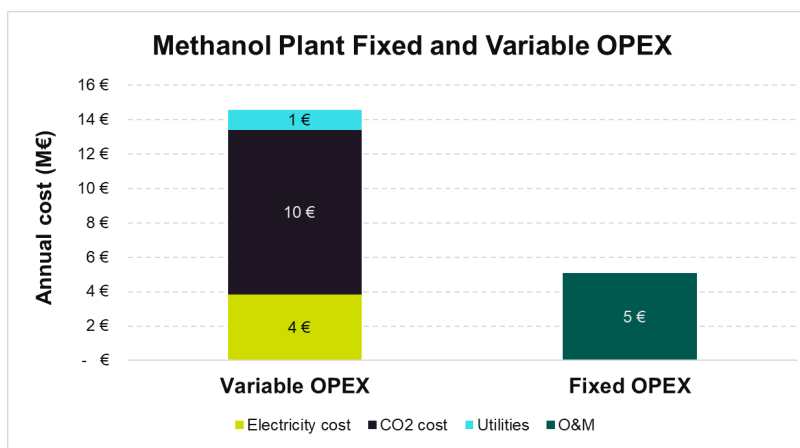


**Figure 16:** Annual Variable and fixed OPEX of the MeOH plant.

with the carbon capture investment and operations cost. The electricity and utilities cost are in total estimated at 5 M€ annually, which is only half of the total annual CO<sub>2</sub> costs. The fixed costs consist of maintenance, insurance, and possible property costs, and are estimated at 5 M€ annually. However, these factors contribute minimally to the whole system’s costs, due to the enormous OPEX costs of the PEM electrolyzer.

### 6.2.3 Levelized Cost of Methanol

The levelized cost of methanol considers both CAPEX and OPEX for the integrated electrolyzer and methanol synthesis system, resulting in a LCOM of 1 100 €/tMeOH. The LCOM indicates the lowest methanol selling price at which the project studied would financially break even at the end of its lifetime. The base case considers only costs, excluding potential revenues from selling excess oxygen and district heating. The impact of potential side-stream revenues is evaluated in the sensitivity analysis. Table 19 shows the LCOM in this study compared to recent market prices of methanol as well as the estimated cost of producing fossil methanol.

**Table 19:** Economic indicators for methanol production.

Parameter	Value	Comment
Methanol selling price (€/tMeOH)	502	5-year average in Europe (Methanex, 2025b)
Cost of fossil methanol production (€/tMeOH)	200–300	Based on IRENA (2021), converted to 2024 EUR
LCOM (€/tMeOH)	1 100	Result of this study

The levelized cost of e-methanol in this case study is more than twice the current market price of methanol, indicating that e-methanol’s competitiveness is highly challenging. Furthermore, when compared to the cost of production by fossil fuels, the e-methanol production is fivefold costlier. The willingness-to-pay by consumers is therefore a crucial but uncertain component. The extreme price disadvantage of

e-methanol should be compensated through regulatory measures or other incentives if its production is to be economically attractive.

However, in the context of the marine sector, the methanol price is also compared to current marine fuels, such as MGO. The energy contents of MeOH and MGO are also considered for comparability. Although the price per unit of mass is similar between methanol and MGO, it is important to note their difference in energy content, which impacts the price per unit of energy. The average global price of marine gas oil is 650 €/tonne in November 2025 (Ship & Bunker, 2025), which translates to a price of 55 €/MWh for MGO. Furthermore, the LCOM is compared with its current e-fuel competitors: e-ammonia, e-gasoline, and e-diesel.

**Table 20:** LCOM in energy-based units compared to alternative options.

Parameter	Value	Unit
LCOM per tonne	1 100	€/t
LCOM per MWh	200	€/MWh
MGO price per tonne	650	€/t
MGO price per MWh	55	€/MWh
e-Ammonia price per tonne	410–1 240	€/t
e-Ammonia price per MWh	79–240	€/MWh
e-Gasoline price per tonne	4 380	€/t
e-Gasoline price per MWh	330–380	€/MWh
e-Diesel price per tonne	3 480	€/t
e-Diesel price per MWh	270–300	€/MWh

Similarly, comparing e-methanol with fossil methanol, e-methanol has major financial disadvantages when compared to MGO. The price per unit of energy is almost four times larger than that MGO, making it extremely uncompetitive in the marine sector currently. This further suggests that regulatory intervention is essential to promote non-fossil alternatives compared to conventional fuels. However, the price range for the competing e-fuels is on similar levels, with e-ammonia showing clear competitiveness. However, e-gasoline and e-diesel are still much more expensive than e-methanol.

## 6.3 Sensitivity Analysis

This section investigates how economic and operational parameters affect the performance and profitability of the integrated e-methanol plant. The analysis quantifies the variations in power price, electrolyzer capital expenses, potential side stream revenues, availability of renewable energy, and carbon tax on the methanol production cost and competitiveness. The results indicate the relative importance of the analyzed factors and propose the parameters that drive the financial viability of the e-methanol plant.

### 6.3.1 Electrolyzer Cost and Electricity Price

The PEM electrolyzer capital expenses for large-scale electrolyzers are highly uncertain, as well as the power prices of the future. Their combined impacts were examined

together. Figure 17 shows how the combinations of different PEM capital expenses and electricity prices could impact the final levelized cost of methanol, assuming no side stream revenues. The electricity price and PEM CAPEX are independent variables. This is illustrated in the figure, which shows that the marginal impact of the PEM CAPEX on the LCOM remains constant across different electricity price levels.

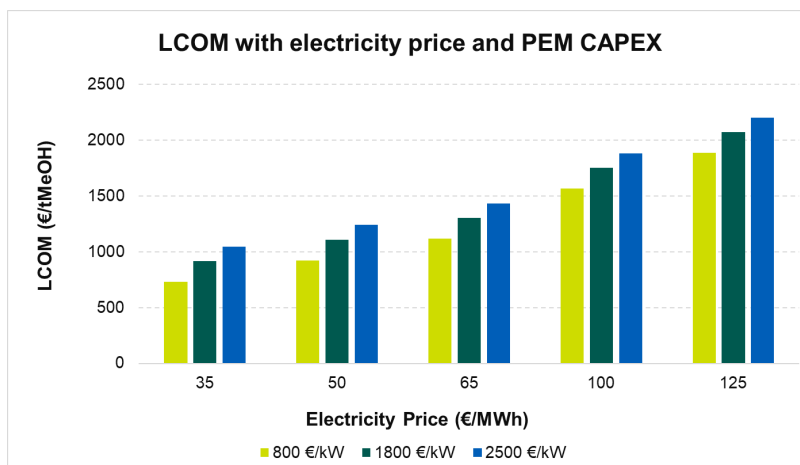


**Figure 17:** PEM Electrolyzer CAPEX and electricity price impact on LCOM.

Although the LCOM responds to changes in the electrolyzer capital expenses, the electricity price is the deciding factor. The figure suggests that the LCOM is highly sensitive to changes in the local electricity price. Table 21 lists the LCOM values for each combination of PEM CAPEX and power price. The table presents that doubling the electricity price, for instance from 50 €/MWh to 100 €/MWh, leads to a 69.2 % increase in the LCOM for the same PEM CAPEX. In contrast, the effect the PEM CAPEX has on the LCOM is less significant. When increasing the PEM CAPEX with more than 200 % and keeping the power price constant, from 800 €/kW to 1 800 €/kW, the LCOM increases by only 26.0 %. These results highlight the importance of power prices in the area where the e-methanol plant is planned.

**Table 21:** The LCOM at different PEM capital expenses and electricity prices.

Electricity price (€/MWh)	PEM CAPEX (€/kW)		
	800	1 800	2,500
35	730	920	1 050
50	925	1 100	1 240
65	1 120	1 300	1 430
100	1 565	1 750	1 880
125	1 890	2 070	2 200

Even with the lowest considered electricity price and PEM CAPEX, the levelized cost is not competitive with the current methanol market price of 502 €/tonne (Methanex, 2025b). The required electricity prices for each of the evaluated PEM CAPEX

alternatives to reach a LCOM equivalent to the current market price are shown in Table 22. The breakeven power prices indicate that even under the optimistic PEM electrolyzer CAPEX, the required electricity cost remains below the current cheapest renewable sources. For instance, the currently cheapest option of onshore wind has a levelized cost of electricity of approximately 30 €/MWh (IRENA, 2025). For the pessimistic PEM CAPEX, the optimal electricity price required to break even was negative. Hence, no feasible solution was found. These findings suggest that electricity remains the bottleneck in finding competitive alternatives to fossil fuels.

**Table 22:** Breakeven electricity price for each PEM scenario.

PEM CAPEX (€/kW)	Breakeven electricity price (€/MWh)
800	18.0
1800	3.80
2500	Not feasible

### 6.3.2 Side Stream Revenues

The simulated process produces excess oxygen and heat, which are considered potential revenue streams. However, the price of oxygen and heat demand throughout the year are uncertain. The impact on the LCOM of the oxygen price and likely demand for the excess heat produced is analyzed.

Table 23 shows the effect of different oxygen market prices on the LCOM. It is assumed that all excess oxygen produced is sold. As the table shows, the oxygen market price does not significantly impact the levelized cost of methanol in this case. For instance, when increasing the price per tonne of oxygen from 25 € to 100 €, the LCOM decreases by 40 €, which is a 4.2 % reduction. Oxygen revenues can therefore be considered as insignificant auxiliary revenue in this case study. Hence, when designing similar plants, the oxygen should be aimed to be produced mainly for consumption within the process, as it yields the most benefit.

**Table 23:** Sensitivity of LCOM to the oxygen selling price.

Oxygen price (€/tO <sub>2</sub> )	Amount sold (t/a)	Total annual revenues (M€)	LCOM (€/tMeOH)
25	158 400	4.0	1 095
50	158 400	8.0	1 080
75	158 400	11.9	1 070
100	158 400	15.8	1 055

The low impact of the oxygen revenue on the LCOM further suggests that investing in an oxyfuel boiler for carbon capture and electrolyzer simultaneously could be carried out for the potential synergies of oxygen utilization. However, as the literature review suggests, there are competing carbon capture technologies to be implemented. Therefore, the choice of carbon capture technology combined with the electrolyzer

should be carefully and critically evaluated before investing. Especially, if the byproduct oxygen flow is excessive and competing carbon capture technologies are less expensive.

For district heating, it is important to note that the available excess heat supply must meet the local demand. If the heat produced by the methanol synthesis process exceeds the demand in the area, the processes will need cooling, which is an expense instead of a revenue.

To conduct the sensitivity analysis, the district heating demand of Helsinki in the year 2024 is used for reference to represent a calendar year of heating demand (Helen Oy, 2025). Figure 18 shows the hourly heating demand and supply from the simulated integrated plant. The excess heat produced by the plant is constant at 140.7 MW throughout the year, while the hourly district heating demand fluctuates. As the figure shows, the excess heat from the e-methanol production process can be considered to match the summertime demand of the reference year. This demonstrates the enormous excess heat supply caused by the simulated process. Therefore, it is appropriate to assume that there may not be sufficient demand for the supplied heat from the e-methanol plant.

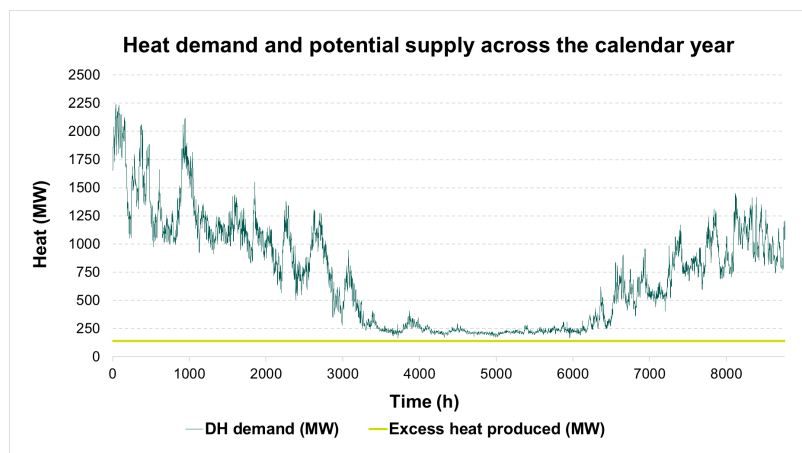


**Figure 18:** District heating demand in 2024 compared to simulated excess heat supply.

Contrary to the potential side stream revenues from oxygen, selling heat to the district heating network could have a significant impact on the LCOM. Table 24 shows the potential revenues for different amounts of heat sold and the effect on the levelized cost of e-methanol. The LCOM shown includes the additional expenses of the cooling needed for each hour when district heating is not sold. As the table shows, selling the excess heat could decrease the competitiveness of the produced methanol by almost 300 €/tMeOH, when compared to the base case LCOM of 1100 €/tMeOH.

The findings of the sensitivity analysis suggest that oxygen could be disregarded as a valuable product, but heating is a treasured byproduct in the context of Nordic countries, where the demand for heating is especially high during the winter months. The simulated exothermic reaction inevitably produces large amounts of excess heat. Locating such a plant in areas where the heat is considered a revenue rather than an

**Table 24:** Sensitivity of LCOM to the district heating selling hours.

District heat demand (h)	Amount sold (MWh/a)	Total revenues (M€/a)	LCOM (€/tMeOH)
2 000	281 400	22.5	1 035
4 000	562 800	45.0	955
6 000	844 200	67.5	880
8 000	1 125 600	90.0	805

expense, could be a deciding factor for its profitability.

### 6.3.3 Renewable Energy Availability

This section evaluates the possibility of powering the integrated electrolyzer and e-methanol plant exclusively with onshore wind power. Table 25 shows the main results of the required capacities and production amounts. To reach the required hydrogen demand of 8.2 tH<sub>2</sub> of the methanol synthesis process, the required capacity of the onshore wind power plant and electrolyzer is 1 180 MW. This is more than double the capacity of the base case, which is estimated at 475 MW. With a capacity of 1 180 MW, the electrolyzer is able to produce the required 65.6 tH<sub>2</sub> annually using only variable onshore wind electricity, while the base case assumed constant energy availability.

**Table 25:** Capacity requirements when using exclusively renewable energy.

Parameter	Value
Wind power plant capacity (MW)	1 190
Annual energy production (GWh/a)	3 900
Annual average wind capacity factor	0.38
Electrolyzer power (MW)	1 180
Hydrogen storage capacity (tH <sub>2</sub> )	11 000

The utilization rate of the electrolyzer would be similar to the wind power capacity factor, which was calculated as 0.38 for the full-year average. In practice, this means that the electrolyzer would be largely oversized and not used at full capacity for majority of the year. Based on the variability in hydrogen production, the estimated storage required for hydrogen is 11.1 tH<sub>2</sub>. With this storage capacity, enough hydrogen could be stored during high-wind hours for use during low-wind hours. To gain a higher utilization rate, the electrolyzer would require another source of electricity or electricity storage in addition to onshore wind power.

The hydrogen production based on available wind power compared to the constant hydrogen demand by the methanol synthesis process is shown in Figure 20. The table shows the intense hourly variation in the produced hydrogen, which is assumed to directly follow the amount of available wind power generation. As can be seen, the variation can be considered seasonal, with less wind during summer months and more

during winter and spring. When the hydrogen production rate is over the hydrogen demand, the storage is charged with excess hydrogen. When the hydrogen production is under the hydrogen demand line, the storage is discharged to meet the hydrogen demand of the methanol production plant.

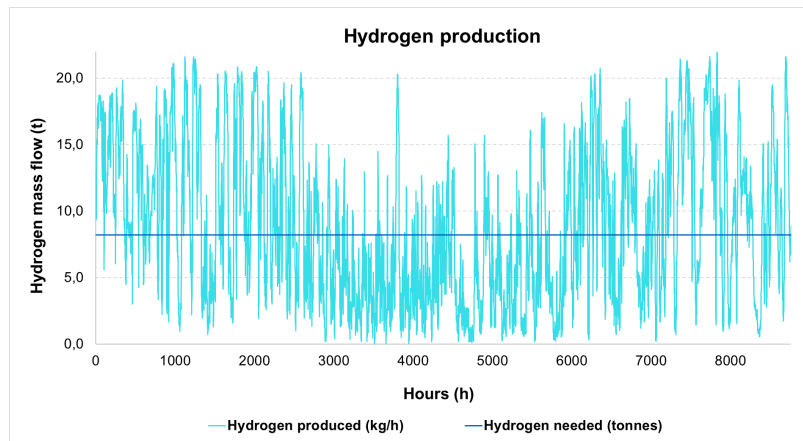


**Figure 19:** Hydrogen production vs. demand.

The fluctuation of oxygen production is assumed to follow the electrolyzer operating hours, similarly as the hydrogen production. However, as the electrolyzer produces eight times more oxygen than hydrogen regarding mass, the fluctuation is considerably more substantial for oxygen production. Figure 20 shows the variation in oxygen production throughout the reference year compared to the demand. The figure also illustrates the eight-fold magnitude of fluctuation for oxygen production compared to the hydrogen production, shown in light blue. The high variability in production can be considered as technically extremely challenging for practical operation of the plant and storage of the gas.

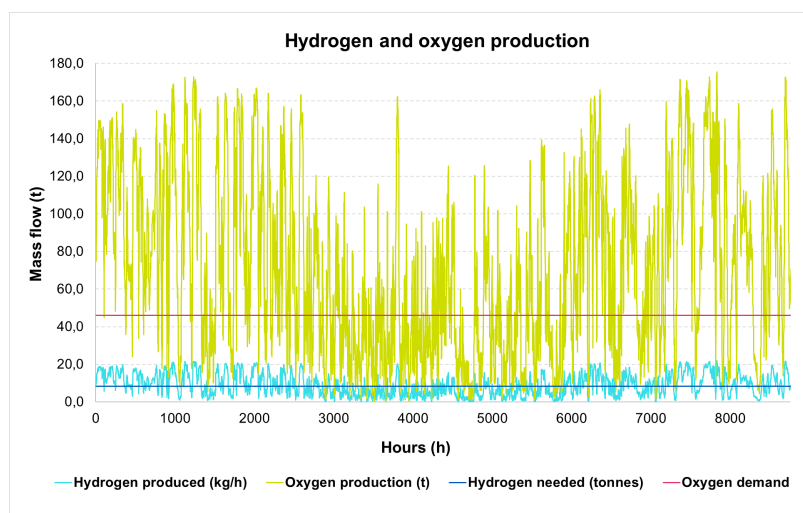


**Figure 20:** Oxygen production vs. demand.

The hydrogen storage ensures a smooth feed of hydrogen to the methanol plant despite the fluctuation in production. Figure 21 shows the cumulative hydrogen inventory in the storage throughout the reference year 2020, starting in September. The production of hydrogen peaks after approximately 4000 hours of operation, when the storage inventory also peaks. After this, the wind power production decreases, leading to smaller hydrogen yields and therefore requiring discharging the hydrogen storage to meet the demand of the methanol plant.

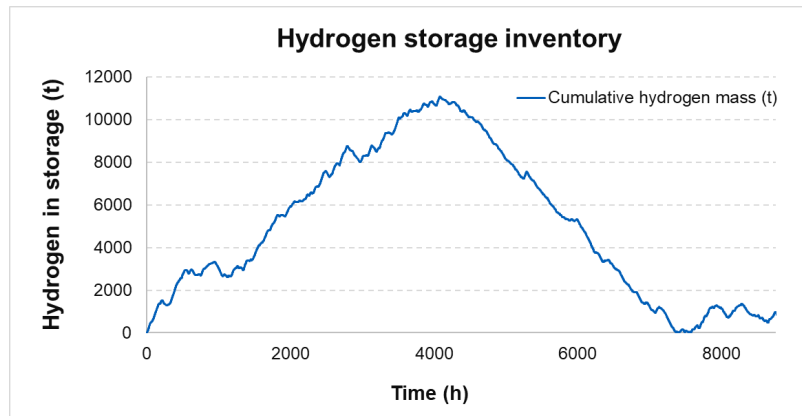


**Figure 21:** Hydrogen storage inventory

The suggested storage capacity is chosen according to the maximum simultaneous storage demand. As a result, the storage would remain underutilized for most of the year, as the cumulative inventory of the storage first increases almost linearly, then decreases similarly. However, the oxygen storage could be more efficient. Figure 22 shows the amount of oxygen storage needed if all excess oxygen were stored.

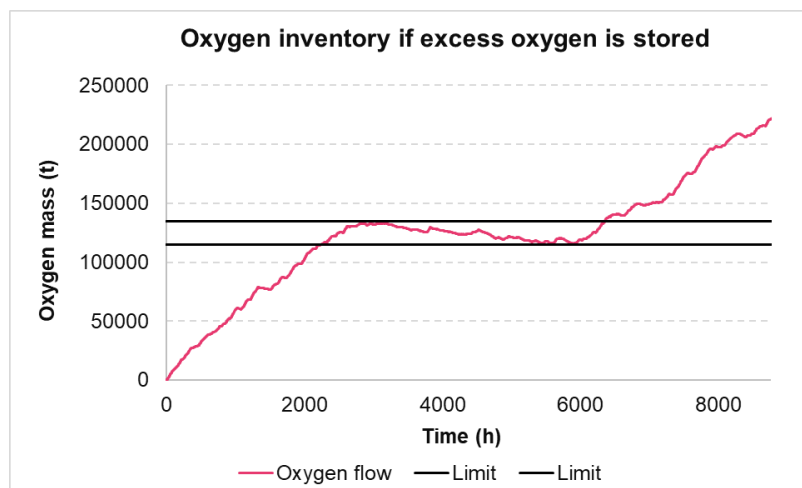


**Figure 22:** Oxygen storage if all excess oxygen was stored

The figure indicates that the needed storage capacity is approximately 20 tonnes. This is illustrated by the downward slope in the figure, which suggests that the oxygen

production is below the demand. The table shows that the oxygen produced by the renewable energy and PEM electrolyzer is excessive for most hours during the year.

The results suggest that relying solely on onshore wind as a power source could significantly decrease the technical and financial efficiency of the plant. The aim of this sensitivity is to demonstrate the challenge in adhering to RFNBO directives while retaining the efficiency and profitability of the plant. However, the actual costs are not estimated in this section, which remains a limitation on the interpretations of the results.

### 6.3.4 Impact of Carbon Tax on Market Prices

This section aims to evaluate the impact of external factors, namely market conditions, on the profitability of e-methanol. In other words, the effect of the carbon tax on the market price of fossil methanol, which competes with renewably sourced e-methanol. Figure 23 compares different possible market prices of fossil methanol and e-methanol. The cost of e-methanol is assumed to stay constant across different carbon taxation levels. The fossil methanol, however, is heavily dependent on the local carbon taxation. The break-even carbon tax found in this study was 340 €/tCO<sub>2</sub>.

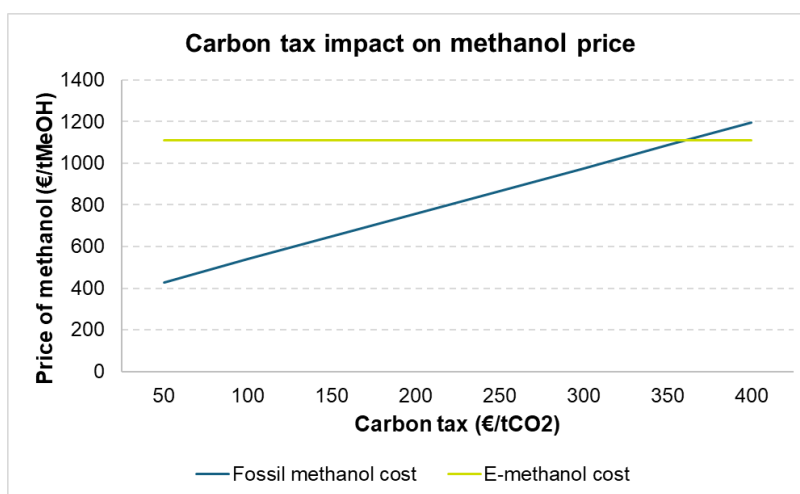


**Figure 23:** Carbon tax and MeOH price

The suggested break-even carbon tax is much higher than current carbon prices. Since 2021, the carbon allowance price under the EU emissions trading system (ETS) has been fluctuating between 60 €/tCO<sub>2</sub> and 90 €/tCO<sub>2</sub>, with some peaks reaching 100 €/tCO<sub>2</sub> (International Carbon Action Partnership, 2025). Reaching 340 €/tCO<sub>2</sub> would require the carbon price to become fivefold its current price, which can be considered a highly ambitious target.

On the other hand, the carbon price under the ETS has been estimated to reach 271-283 €/tCO<sub>2</sub> or up to 360 €/tCO<sub>2</sub> under the ETS2 by 2030 (Abrell et al., 2024; Günther et al., 2025). As the future market for methanol can be considered unsettled, the sector, and therefore which ETS scheme it will fall under, is uncertain. However, the higher

end of the estimations by Abrell et al. (2024) and Günther et al. (2025) indicates that a higher carbon tax is necessary for the EU to reach its climate targets by 2030. Consequently, e-methanol has the possibility to become financially feasible compared to fossil methanol.

## 6.4 Limitations and Suggestions for Further Research

There are a few possible limitations that may have affected the results of this study. The thesis is a system-level analysis of e-methanol production from a technical and economic perspective. The broad focus of the topic may have led to relevant details being omitted or overlooked to achieve a comprehensive whole. The most significant details that might impact the results are the inputs of the simulation model or economic assumptions.

The time limit for the study was six months, which defined the initial scope of the work. Regarding technical details, the electrolyzer and e-methanol models were developed using thermodynamic balances, assuming total stoichiometric conversion, which represents the theoretical maximum efficiency. In reality, the results may not achieve the theoretical maximum. For more exact estimations on the reactions, conversions, and yields of the process, further research could consider implementing a kinetic model in the simulation.

Furthermore, the Aspen model is not mathematically optimized according to cost or technical efficiency, but rather represents one efficient solution for the process. The exact optimum for the process was not targeted in this study, as the focus was on a comprehensive techno-economic evaluation of a possible solution. With a more thorough mathematical or iterative analysis of the optimal pressures and temperatures for the blocks within the model, the methanol yield could be further increased or maximized.

Regarding the financial analysis, some assumptions were made that may entail possible limitations. The scaling of equipment cost used a formula and scaling factor used in general in industry. In reality, the economies of scale may behave differently than assumed. The modeled equipment prices may therefore differ from reality.

To better understand the real market potential of e-methanol, conducting a market analysis on the willingness to pay a premium for carbon-free methanol could be beneficial. Critically assessing the levelized costs by considering incentives, such as subsidies from the European Union, could further increase insight into possible profits available from such projects.

Finally, this study is modeled according to the aim to achieve the highest possible CO<sub>2</sub> utilization rate. Analyzing the process only from one perspective regarding the design and sizing can be considered a limitation. The benefits of maximizing CO<sub>2</sub> utilization include lower environmental impacts from production and achievable economies of scale from large-scale production. However, this perspective may pose limitations on the financial feasibility. Therefore, for future research, it could be beneficial to explore

different points of focus for the optimization. For instance, to size the electrolyzer according to the oxyfuel boiler's demand.

## 7 Conclusions

This thesis aimed to identify efficient pathways and associated costs of e-methanol production through oxyfuel carbon capture and hydrogen production. This study identified several efficient pathways for producing hydrogen through electrolysis and methanol synthesis.

The production process was evaluated through simulation of an e-methanol synthesis plant and PEM electrolyzer in Aspen Plus. The process model included heat integration and considered excess heat and oxygen production as possible side-stream revenue sources. The costs of e-methanol production were estimated using the levelized cost method, by dividing the discounted total costs over the plant lifetime by the discounted total production of e-methanol. The levelized cost of methanol was critically reviewed through sensitivity analysis on the electrolyzer capital expenditures, electricity prices, and renewable electricity availability.

Based on the technical and economic models, it can be concluded that e-methanol production is not financially competitive with current fossil methanol, as e-methanol costs more than twice as much as its fossil alternative. The main findings were that with an annual production of 300 ktMeOH of 99.4 % purity, the levelized cost of methanol is 1 100 €/tMeOH. This value is in line with the LCOM estimations by, for instance IRENA (2021). The results show that the process is highly sensitive to local power prices and to the capital expenditures required for the electrolyzer.

The sensitivity analysis revealed that oxygen is not a valuable byproduct, but selling excess heat from the process can significantly decrease the LCOM. Furthermore, the variable availability of renewable electricity is a challenge for continuous hydrogen production. Therefore, the alternative solutions for storage should be further investigated. In practice, it should be evaluated whether it is more economically feasible to store hydrogen or, alternatively, electricity in batteries, to be used in the e-methanol production process.

The simulation was based on the carbon dioxide emissions from an existing 60 MWe biomass combined heat and power plant. While the approach limits the generalizability of the results, the case study provides new insight into the technical feasibility of carbon capture and utilization in the context of large-scale biomass power plants. Furthermore, the levelized cost model provides a valuable understanding of the state-of-the-art costs and competitiveness of e-methanol production through the oxyfuel and electrolyzer pathway. This approach enabled the identification of synergies within the production process and the utilization of waste byproducts and heat.

This work has estimated the associated costs of integrating the synergies from variable renewable energy and decarbonizing hard-to-abate sectors. It has critically evaluated various carbon capture and hydrogen production technologies to be combined with a biomass heat and power plant. Furthermore, a suggestion for an e-methanol plant configuration was designed, simulated, and presented. Overall, this study demonstrates the techno-economic potential of producing e-methanol and provides one pathway for

decarbonization in hard-to-abate sectors.

## References

- Abrell, J., Bilici, S., Blesl, M., Fahl, U., Kattelmann, F., Kittel, L., Kosch, M., Luderer, G., Marmullaku, D., Pahle, M., Pietzcker, R., Rodrigues, R. and Siegle, J. (2024), 'Optimal allocation of the EU carbon budget: A multi-model assessment', *Energy Strategy Reviews* **51**, 101271.  
**URL:** <https://www.sciencedirect.com/science/article/pii/S2211467X23002213>
- Agyekum, E. B., Sun, H., Kemausuor, F. and Afrane, S. (2025), 'E-methanol: a sustainable fuel with a promising role in the energy transition', *Carbon Research* **4**(4).  
**URL:** <https://doi.org/10.1007/s44246-024-00179-0>
- Air Liquide (2017), Standard Plants: Air Separation and Gas Processing Units, Technical brochure, Air Liquide Engineering & Construction, Paris, France. Available as PDF via AirLiquide Engineering & Construction website.  
**URL:** <https://engineering.airliquide.com/sites/engineering/files/2022-09/air-liquide-e-c-standard-plants-september-2017.pdf>
- Akyüz, E. S., Telli, E. and Farsak, M. (2024), 'Hydrogen generation electrolyzers: Paving the way for sustainable energy', *International Journal of Hydrogen Energy* **81**, 1338–1362.  
**URL:** <https://www.sciencedirect.com/science/article/pii/S0360319924028490>
- Alrebei, O. F., Amhamed, A. I., El-Naas, M. H., Hayajnh, M., Orabi, Y. A., Fawaz, W., Al-tawaha, A. S. and Medina, A. V. (2022), 'State of the art in separation processes for alternative working fluids in clean and efficient power generation', *Separations* **9**(1).  
**URL:** <https://www.mdpi.com/2297-8739/9/1/14>
- Aminaho, E. N., Aminaho, N. S. and Aminaho, F. (2025), 'Techno-economic assessments of electrolyzers for hydrogen production', *Applied Energy* **399**, 126515.  
**URL:** <https://www.sciencedirect.com/science/article/pii/S0306261925012450>
- Aronietis, R., Sys, C., van Hassel, E. and Vanelslander, T. (2016), 'Forecasting port-level demand for lng as a ship fuel: the case of the port of antwerp', *Journal of Shipping and Trade* **1**.
- Badgett, A., Brauch, J., Thatte, A., Rubin, R., Skangos, C., Wang, X., Ahluwalia, R., Pivovar, B. and Ruth, M. (2024), Updated manufactured cost analysis for proton exchange membrane water electrolyzers, Technical Report NREL/TP-6A20-87625, National Renewable Energy Laboratory. Golden, CO.  
**URL:** <https://docs.nrel.gov/docs/fy24osti/87625.pdf>
- Barbir, F. (2005), 'Pem electrolysis for production of hydrogen from renewable energy sources', *Solar Energy* **78**(5), 661–669. Solar Hydrogen.  
**URL:** <https://www.sciencedirect.com/science/article/pii/S0038092X04002464>
- Belaissaoui, B., Le Moullec, Y., Hagi, H. and Favre, E. (2014), 'Energy efficiency of oxygen enriched air production technologies: Cryogeny vs membranes', *Separation*

- and Purification Technology **125**, 142–150.  
**URL:** <https://www.sciencedirect.com/science/article/pii/S1383586614000768>
- Brigagão, G. V., de Medeiros, J. L. and de Queiroz F. Araújo, O. (2025), ‘Landfill-gas oxy-combustion via novel air separation unit: Upgraded exergy performance’, *Renewable and Sustainable Energy Reviews* **211**, 115309.  
**URL:** <https://www.sciencedirect.com/science/article/pii/S1364032124010359>
- Cai, R., Krzystowczyk, E., Braunberger, B., Li, F. and Neal, L. (2024), ‘Techno-economic analysis of chemical looping air separation using a perovskite oxide sorbent’, *International Journal of Greenhouse Gas Control* **132**, 104070.  
**URL:** <https://www.sciencedirect.com/science/article/pii/S1750583624000136>
- Centi, G., Quadrelli, E. A. and Perathoner, S. (2013), ‘Catalysis for CO<sub>2</sub> conversion: a key technology for rapid introduction of renewable energy in the value chain of chemical industries’, *Energy & Environmental Science* **6**(6), 1711–1731.
- Cesaro, Z., Ives, M., Nayak-Luke, R., Mason, M. and Bañares-Alcántara, R. (2021), ‘Ammonia to power: Forecasting the levelized cost of electricity from green ammonia in large-scale power plants’, *Applied Energy* **282**, 116009.
- Choi, Y., Sim, G. D., Jung, U., Park, Y., Youn, M. H., Chun, D. H., Rhim, G. B., Kim, K. Y. and Koo, K. Y. (2024), ‘Copper catalysts for CO<sub>2</sub> hydrogenation to CO through reverse water–gas shift reaction for e-fuel production: Fundamentals, recent advances, and prospects’, *Chemical Engineering Journal* **492**, 152283.
- Collodi, G., Azzaro, G., Ferrari, N. and Santos, S. (2017), ‘Demonstrating large scale industrial ccs through ccu – a case study for methanol production’, *Energy Procedia* **114**, 122–138. 13th International Conference on Greenhouse Gas Control Technologies, GHGT-13, 14-18 November 2016, Lausanne, Switzerland.  
**URL:** <https://www.sciencedirect.com/science/article/pii/S1876610217313280>
- Deloitte (2021), ‘Fueling the future of mobility: Hydrogen electrolyzers’. White paper.  
**URL:** <https://www.deloitte.com/content/dam/assets-zone2/fr/no-index/docs/services/consulting/2024/fueling-the-future-of-mobility-hydrogen-electrolyzers.pdf>
- Eckl, F., Moita, A., Castro, R. and Neto, R. C. (2025), ‘Valorization of the by-product oxygen from green hydrogen production: A review’, *Applied Energy* **378**, 124817.  
**URL:** <https://www.sciencedirect.com/science/article/pii/S0306261924022001>
- Energiateglisu ry (2025), ‘Kaukolämmön hinta – tilastotiedot’, <https://energia.fi/tilastot/kaukolampotilastot/kaukolammon-hinta/>. Accessed: 2025-11-28.
- European Commission (2023), ‘Commission delegated regulation (eu) 2023/1184 of 10 february 2023 supplementing directive (eu) 2018/2001 by establishing a union methodology on renewable liquid and gaseous transport fuels of non-biological origin’, Official Journal of the European Union, L 157, 11–19 (20 June 2023).

- URL:** <https://eur-lex.europa.eu/legal-content/EN/TXT/?uri=uriserv:OJ.L.2023.157.01.0011.01.ENG>
- European Commission (2025), ‘Renewable hydrogen’. Accessed: 2025-12-15.  
**URL:** [https://energy.ec.europa.eu/topics/eus-energy-system/hydrogen/renewable-hydrogen\\_en](https://energy.ec.europa.eu/topics/eus-energy-system/hydrogen/renewable-hydrogen_en)
- European Environment Agency (2025), ‘Eea greenhouse gases — data viewer’, <https://www.eea.europa.eu/data-and-maps/data/data-viewers/greenhouse-gases-viewer>. Accessed 1 Dec 2025.
- European Hydrogen Observatory (2025a), Electrolyser cost, Technical report, European Hydrogen Observatory. Accessed: 2025-11-20.  
**URL:** <https://ipcei.observatory.clean-hydrogen.europa.eu/hydrogen-landscape/production-trade-and-cost/electrolyser-cost>
- European Hydrogen Observatory (2025b), ‘Hydrogen production and consumption projects’, <https://observatory.clean-hydrogen.europa.eu/hydrogen-landscape/projects-and-valleys/hydrogen-production-and-consumption-projects>. accessed May 2025.
- European Union (2021), ‘Regulation (eu) 2021/1119’. note.  
**URL:** <https://eur-lex.europa.eu/eli/reg/2023/839/oj>
- European Union (2023), ‘Commission delegated regulation (eu) 2023/1184 of 10 february 2023 supplementing directive (eu) 2018/2001 by establishing a union methodology setting out detailed rules for the production of renewable liquid and gaseous transport fuels of non-biological origin’, Official Journal of the European Union, L 157, 20 June 2023. Accessed 11 December 2025.  
**URL:** [https://eur-lex.europa.eu/eli/reg\\_diel/2023/1184/oj/eng](https://eur-lex.europa.eu/eli/reg_diel/2023/1184/oj/eng)
- Eurostat (2025), ‘Electricity price statistics: Electricity prices for non-household consumers’, [https://ec.europa.eu/eurostat/statistics-explained/index.php?title=Electricity\\_price\\_statistics#Electricity\\_prices\\_for\\_non-household\\_consumers](https://ec.europa.eu/eurostat/statistics-explained/index.php?title=Electricity_price_statistics#Electricity_prices_for_non-household_consumers). accessed 26 November 2025.
- Fingrid Oyj (2025), ‘Total production capacity used in the wind power forecast, hourly, dataset id 268’, <https://data.fingrid.fi/en/datasets/268>. Accessed: 2025-12-04.
- Friedrichs-Schucht, M., Hasché, F. and Oezaslan, M. (2024), ‘Water crossover in proton exchange membrane water electrolysis’, *Journal of The Electrochemical Society* **171**(7), 074512.  
**URL:** <https://iopscience.iop.org/article/10.1149/1945-7111/ad6213>
- Gelten, H., Hajimolana, Y., de Jong, W., Heesink, B., Nami, H., Aalderink, B. and van Leeuwen, R. (2026), ‘Power-to-methanol: Techno-economic analysis of a regional, decentral case-study’, *Fuel* **405**, 136528.  
**URL:** <https://www.sciencedirect.com/science/article/pii/S0016236125022537>

- Gulay, E. D., Ozgur Colpan, C. and Ezan, M. A. (2025), ‘Techno-economic assessment of green hydrogen production in izmir: Evaluating electrolyzer technologies, modularization strategies, and renewable energy integration’, *Energy Conversion and Management* **333**, 119797.  
**URL:** <https://www.sciencedirect.com/science/article/pii/S0196890425003206>
- Günther, C., Pahle, M., Govorukha, K., Osorio, S. and Fotiou, T. (2025), ‘Carbon prices on the rise? shedding light on the emerging second EU emissions trading system (EU ETS 2)’, *Climate Policy* pp. 1–12.
- Hamedani, E. A., Yajloo, A. B. and Talebi, S. (2025), ‘A comprehensive review on carbon capture, transportation, storage, and utilization technologies; part I: Carbon capture technologies’, *AEST* pp. 119–132.
- Hamelinck, C. and Bunse, M. (2022), ‘Carbon footprint of methanol’, Report commissioned by the Methanol Institute; studio Gear Up, Amsterdam. Carbon footprint assessment of methanol: lifecycle study of various production pathways (Jan 2022).  
**URL:** [https://www.studiogearup.com/wp-content/uploads/2022/02/2022\\_GU\\_for\\_MIMethanol\\_carbon\\_footprint\\_DEF\\_1.pdf](https://www.studiogearup.com/wp-content/uploads/2022/02/2022_GU_for_MIMethanol_carbon_footprint_DEF_1.pdf)
- Helen Oy (2025), ‘Avoin data – helsingin kaukolämmön tuntiteho 2015–2024’, <https://www.helen.fi/tietoa-meista/helen/avoindata>. Accessed: 2025-11-28.
- Higginbotham, P., White, V., Fogash, K. and Guvelioglu, G. (2011), ‘Oxygen supply for oxyfuel co2 capture’, *International Journal of Greenhouse Gas Control* **5**, S194–S203. Oxyfuel Combustion Technology - Working Toward Demonstration and Commercialisation.  
**URL:** <https://www.sciencedirect.com/science/article/pii/S1750583611000375>
- Huang, X., Ai, N., Li, L., Jiang, Q., Wang, Q., Ren, J. and Wang, J. (2022), ‘Simulation of CO2 capture process in flue gas from oxy-fuel combustion plant and effects of properties of absorbent’, *Separations* **9**(4), 95.
- Hurskainen, M. (2017), Industrial oxygen demand in finland, Technical Report VTT-R-06563-17, VTT Technical Research Centre of Finland. Accessed: 2025-11-28.  
**URL:** <https://publications.vtt.fi/julkaisut/muut/2017/VTT-R-06563-17.pdf>
- IEA (2022), ‘Direct air capture 2022 – executive summary’, <https://www.iea.org/reports/direct-air-capture-2022/executive-summary>. Accessed: 2025-07-29.
- IEA (2024), ‘Renewables 2024: Analysis and forecast to 2029’. Accessed: 2025-07-25.  
**URL:** <https://iea.blob.core.windows.net/assets/17033b62-07a5-4144-8dd0-651cdb6caa24/Renewables2024.pdf>
- International Carbon Action Partnership (2025), ‘Icap allowance price explorer’, <https://icapcarbonaction.com/en/ets-prices>. Accessed: 2025-12-10.
- IRENA (2021), ‘Innovation Outlook: Renewable Methanol’. Accessed: 2025-07-25.  
**URL:** <https://www.methanol.org/renewable/>

- IRENA (2025), 'Renewable power generation costs in 2024', [https://www.irena.org/-/media/Files/IRENA/Agency/Publication/2025/Jul/IRENA\\_TEC\\_RPGC\\_in\\_2024\\_2025.pdf](https://www.irena.org/-/media/Files/IRENA/Agency/Publication/2025/Jul/IRENA_TEC_RPGC_in_2024_2025.pdf). Accessed 26 November 2025; ISBN 978-92-9260-669-5.
- Jha, M. and Gaur, N. (2022), 'Life cycle of medical oxygen from production to consumption', *Journal of Family Medicine and Primary Care* **11**(4), 1231–1236.
- Jung, C. and Schindler, D. (2020), 'The annual cycle and intra-annual variability of the global wind power distribution estimated by the system of wind speed distributions', *Sustainable Energy Technologies and Assessments* **42**, 100852.  
**URL:** <https://www.sciencedirect.com/science/article/pii/S2213138820312790>
- Kato, T., Kubota, M., Kobayashi, N. and Suzuoki, Y. (2005), 'Effective utilization of by-product oxygen from electrolysis hydrogen production', *Energy* **30**(14), 2580–2595. International Energy Workshop.  
**URL:** <https://www.sciencedirect.com/science/article/pii/S0360544204003123>
- Kiss, A. A., Pragt, J. J., Vos, H. J., Bargeman, G. and de Groot, M. T. (2016), 'Novel efficient process for methanol synthesis by co<sub>2</sub> hydrogenation', *Chemical Engineering Journal* **284**, 260–269.
- Kumar, S., Somanna, V., Thakur, J. and Gunasekara, S. N. (2025), 'Exploring excess heat recovery in proton exchange membrane electrolysis for green hydrogen production: A technical and economic analysis', *Energy Conversion and Management* **342**, 120118.  
**URL:** <https://www.sciencedirect.com/science/article/pii/S0196890425006429>
- Leonzio, G., Zondervan, E. and Foscolo, P. U. (2019), 'Methanol production by co<sub>2</sub> hydrogenation: Analysis and simulation of reactor performance', *International Journal of Hydrogen Energy* **44**(16), 7915–7933.
- Li, R., Xin, T., Xu, H., Ou, Z., Liu, Y. and Xu, C. (2024), 'Thermodynamic analysis of the air separation unit and co<sub>2</sub> purification unit in the semi-closed supercritical co<sub>2</sub> cycle with nearly zero emission', *Fuel* **378**, 132952.  
**URL:** <https://www.sciencedirect.com/science/article/pii/S001623612402101X>
- Liski, M. and Vehviläinen, I. (2016), 'Gone with the wind? an empirical analysis of the renewable energy rent transfer', Working Paper 6250, CESifo. Category 10: Energy and Climate Economics; ISSN 2364-1428. Also available via SSRN and RePEc [1, 2].  
**URL:** [Twww.CESifo-group.org/wp](http://www.CESifo-group.org/wp) T
- Lube, B., Perz, E., Sanz, W. and 6th Edition of the European Conference on Supercritical CO<sub>2</sub> (sCO<sub>2</sub>) for Energy Systems April 09–11, 2025, Delft, Netherlands (2025), 'Thermodynamic comparison of cryogenic and membrane oxygen production for the supercritical net power cycle', *6th Edition of the European Conference on Supercritical CO<sub>2</sub> (sCO<sub>2</sub>) for Energy Systems: April 09–11, 2025, Delft, The Netherlands* pp. 99–111.

- Marques, L., Vieira, M., Condeço, J., Henriques, C. and Mateus, M. (2024), 'A Mini-Review on Recent Developments and Improvements in CO<sub>2</sub> Catalytic Conversion to Methanol: Prospects for the Cement Plant Industry', *Energies* **17**(21), 5285.
- Mehrpooya, M., Golestani, B. and Ali Mousavian, S. (2020), 'Novel cryogenic argon recovery from the air separation unit integrated with lng regasification and co<sub>2</sub> transcritical power cycle', *Sustainable Energy Technologies and Assessments* **40**, 100767.  
**URL:** <https://www.sciencedirect.com/science/article/pii/S2213138820301351>
- Methanex (2025a), 'Methanol investor presentation'. January 2025.  
**URL:** <https://www.methanex.com/wp-content/uploads/MEOH-Investor-Presentation-Jan-2025.pdf>
- Methanex (2025b), 'Methanol pricing – our products · about methanol', <https://www.methanex.com/about-methanol/pricing/>. Accessed: 2025-11-27.
- Methanol Institute (2016), Physical properties of pure methanol, Technical report, Methanol Institute. Online PDF.  
**URL:** <https://methanol.org/wp-content/uploads/2016/06/Physical-Properties-of-Pure-Methanol.pdf>
- Micari, M. and Agrawal, K. V. (2022), 'Oxygen enrichment of air: Performance guidelines for membranes based on techno-economic assessment', *Journal of Membrane Science* **641**, 119883.  
**URL:** <https://www.sciencedirect.com/science/article/pii/S0376738821008267>
- Nema, A., Kumar, A. and Warudkar, V. (2025), 'An in-depth critical review of different carbon capture techniques: Assessing their effectiveness and role in reducing climate change emissions', *Energy Conversion and Management* **323**, 119244.
- Niu, Y., Zeng, X., Xia, J. et al. (2025), 'Recent progress of green hydrogen production technology', *Frontiers of Chemical Science and Engineering* **19**, 93. Accessed via Aalto University Library proxy.  
**URL:** <https://doi.org/10.1007/s11705-025-2551-4>
- Nyári, J., Magdeldin, M., Larimi, M., Järvinen, M. and Santasalo-Aarnio, A. (2020), 'Techno-economic barriers of an industrial-scale methanol ccu-plant', *Journal of CO<sub>2</sub> Utilization* **39**, 101166.  
**URL:** <https://www.sciencedirect.com/science/article/pii/S2212982020300688>
- Obi, D., Onyekuru, S. and Orga, A. (2025), 'Minimizing carbon capture costs in power plants: A novel dimensional analysis framework for techno-economic evaluation of oxyfuel combustion, pre-combustion, and post-combustion capture systems', *Energy Science & Engineering* **4**.  
**URL:** <https://scijournals.onlinelibrary.wiley.com/doi/10.1002/ese3.2089>
- Ong, C. W., Lin, J.-X., Tsai, M.-L., Thoe, K. S. and Chen, C.-L. (2024), 'Techno-economic and carbon emission analyses of a methanol-based international renewable

- energy supply chain', *International Journal of Hydrogen Energy* **49**, 1572–1585.  
**URL:** <https://www.sciencedirect.com/science/article/pii/S0360319923053399>
- Pérez-Fortes, M., Schöneberger, J. C., Boulamanti, A. and Tzimas, E. (2016), 'Methanol synthesis using captured CO<sub>2</sub> as raw material: Techno-economic and environmental assessment', *Applied Energy* **161**, 718–732.
- Pratama, M. R., Muthia, R. and Purwanto, W. W. (2023), 'Techno-economic and life cycle assessment of the integration of bioenergy with carbon capture and storage in the polygeneration system (beccs-ps) for producing green electricity and methanol', *Carbon Neutrality* **2**(26).  
**URL:** <https://link.springer.com/article/10.1007/s43979-023-00069-1>
- Prašnikar, A. and Likozar, B. (2022), 'Sulphur poisoning, water vapour and nitrogen dilution effects on copper-based catalysts', *Reaction Chemistry Engineering*. RSC Reaction Engineering, detailed study on impurity effects (sulphur, water, N) on Cu-based CO hydrogenation catalysts.
- Ravi, S. S., Mazumder, J., Sun, J., Brace, C. and Turner, J. W. G. (2023), 'Techno-economic assessment of synthetic e-fuels derived from atmospheric CO<sub>2</sub> and green hydrogen', *Energy Conversion and Management* **291**, 117271.
- Rivera-Tinoco, R., Farran, M., Bouallou, C., Auprêtre, F., Valentin, S., Millet, P. and Ngameni, J. (2016), 'Investigation of power-to-methanol processes coupling electrolytic hydrogen production and catalytic CO<sub>2</sub> reduction', *International Journal of Hydrogen Energy* **41**(8), 4546–4559.  
**URL:** <https://www.sciencedirect.com/science/article/pii/S0360319915309605>
- Ruland, T. e. a. (2020), 'CO<sub>2</sub> hydrogenation with Cu/ZnO/Al<sub>2</sub>O<sub>3</sub>: A benchmark study', *ChemCatChem*. Published online in ChemCatChem; investigate industrial Cu-based catalyst for methanol synthesis from CO hydrogenation.
- Şahin, M. E. (2024), 'An overview of different water electrolyzer types for hydrogen production', *Energies* **17**(19).  
**URL:** <https://www.mdpi.com/1996-1073/17/19/4944>
- Samimi, F., Rahimpour, M. R. and Shariati, A. (2017), 'Development of an Efficient Methanol Production Process for Direct CO<sub>2</sub> Hydrogenation over a Cu/ZnO/Al<sub>2</sub>O<sub>3</sub> Catalyst', *Catalysts* **2017**, Vol. 7, Page 332 **7**(11), 332.  
**URL:** <https://www.mdpi.com/2073-4344/7/11/332/htm>  
<https://www.mdpi.com/2073-4344/7/11/332>
- Ship & Bunker (2025), 'Average bunker fuel prices – mgo and other marine fuels', <https://shipandbunker.com/prices#MGO>. Accessed: 2025-12-03.
- Sillman, J., Ylä-Kujala, A., Hyypiä, J., Kärri, T., Tuomaala, M. and Soukka, R. (2025), 'Feasibility assessment of e-methanol value chains: Temporal and regional renewable energy, costs, and climate impacts', *Applied Energy* **391**, 125887.  
**URL:** <https://www.sciencedirect.com/science/article/pii/S03606261925006178>

- Skorek-Osikowska, A., Łukasz Bartela and Kotowicz, J. (2017), 'Thermodynamic and ecological assessment of selected coal-fired power plants integrated with carbon dioxide capture', *Applied Energy* **200**, 73–88.  
**URL:** <https://www.sciencedirect.com/science/article/pii/S0306261917305238>
- Sollai, S., Porcu, A., Tola, V., Ferrara, F. and Pettinau, A. (2023), 'Renewable methanol production from green hydrogen and captured co<sub>2</sub>: A techno-economic assessment', *Journal of CO<sub>2</sub> Utilization* **68**, 102345.
- Souissi, N. (2024), Fueling the future: A techno-economic evaluation of e-ammonia production for marine applications, Oies paper et40, Oxford Institute for Energy Studies.  
**URL:** <https://www.oxfordenergy.org/wpcms/wp-content/uploads/2024/10/ET40-Fuelling-the-future-final.pdf>
- Spoof-Tuomi, K. and Manfo, T. A. (2025), 'Techno-economic analysis of green hydrogen production – 20 mw pem electrolysis plant: report on task 1.3 & 1.4'. Part of the "Hydrogen economy in the food system" project.